



UNICA

UNIVERSITÀ  
DEGLI STUDI  
DI CAGLIARI



Università di Cagliari

UNICA IRIS Institutional Research Information System

**This is the Author's [accepted] manuscript version of the following contribution:**

Marie Pierre Dabard, Alfredo Loi, Pamela Pavanetto, Mattia Alessio Meloni, Natalia Hauser, Massimo Matteini, Antonio Funedda, 2021. Provenance of Ediacaran- Ordovician sediments of the Medio Armorican Domain, Brittany, West France: Constraints from U/Pb detrital zircon and Sm–Nd isotope data. *Gondwana Research* 90, 63–76.

**The publisher's version is available at:**

[https:// doi. org/ 10. 1016/j. gr. 2020. 11. 004](https://doi.org/10.1016/j.jgr.2020.11.004)

**When citing, please refer to the published version.**

30 **Provenance of Ediacaran-Ordovician sediments of the Medio Armorican Domain, Brittany,**  
31 **West France: Constraints from U/Pb detrital zircon and Sm-Nd isotope data**

32 Marie Pierre Dabard<sup>†, a</sup>, Alfredo Loi<sup>b\*</sup>, Pamela Pavanetto<sup>b, c</sup>, Mattia Alessio Meloni<sup>b</sup>, Natalia Hauser<sup>d</sup>,  
33 Massimo Matteini<sup>d</sup>, Antonio Funedda<sup>b</sup>

34 a: Géosciences UMR6118 CNRS/Université Rennes1, Campus de Beaulieu, 35042 Rennes Cédex,  
35 France

36 b: University of Cagliari Department of Chemical and Geological Sciences, Cittadella Universitaria,  
37 Blocco A - 09042 Monserrato (Italy)

38 c: Instituto de Geografia, Federal University of Uberlândia (UFU), Campus Monte Carmelo, 38500-  
39 000, MG, Brazil

40 d: Laboratory of Geochronology and Isotope Geochemistry, Instituto de Geociências, Universidade  
41 de Brasília (UnB), Brasília-DF 70910-900, Brazil

42 †: Deceased

43 \*: Corresponding author. E-mail address: [alfloi@unica.it](mailto:alfloi@unica.it) (A. Loi)

44

45 **Abstract**

46 The temporal evolution of the sedimentary source areas of the Armorican Massif, involving  
47 Ediacaran to Upper Ordovician strata, is investigated to discuss paleogeographic affinities and  
48 changes that occurred as a result of the Cadomian orogenesis. Until now, paleogeographic  
49 reconstructions based on geodynamic, stratigraphic and palaeontological data show a geological  
50 continuity between the Armorican Massif and the Iberian and Bohemian massifs, and allow to locate  
51 the Armorican Massif near the West African Craton and the Trans-Saharan Belt. This study goes  
52 beyond the interpretations based on lithostratigraphic correlation, which may be influenced by the  
53 allocyclic factors (e.g., sea level change) or fauna assemblages that have a wide provincial  
54 distribution, in order to provide a correct assessment of sediment flux. In order to provide a more  
55 accurate paleogeographic location, the provenance of the siliciclastic sediments has been studied  
56 using U-Pb LA-MC-ICP-MS geochronology on detrital zircons coupled with whole-rock Sm-Nd and  
57 zircon Lu-Hf isotope analysis. This work was done on the sedimentary succession of the Crozon  
58 Peninsula (Medio Armorican Domain) that shows the tectonic evolution of northern Gondwana from  
59 Neoproterozoic to Palaeozoic times. The oldest studied sedimentary rocks belong to the Brioverian  
60 succession that contains mainly 519 to 781 Ma old zircons, likely derived from sources still present

61 in the Armorican basement. Subsequently, in the rift stages of the Rheic Ocean, the lower Palaeozoic  
62 succession was deposited, with contributions from, a new source of 827 to 1,120 Ma old zircons.

63 The comparison of the zircon populations shows increased of negative  $\epsilon_{\text{Nd}(t)}$  and  $\epsilon_{\text{Hf}(t)}$  values of  
64 the sedimentary supply in the post-Cadomian samples. Moreover, it allows to recognize that the  
65 Medio and North Armorican domains had different locations during the Lower Ordovician, and some  
66 areas of the Iberian Massif and the Medio Armorican Domain were contiguous close to the Sahara  
67 Metacraton and Arabian-Nubian Shield.

68

69

70 **Key words:** North Gondwana; Cadomian Belt; Brioverian; Grès Armorican Formation; U-Pb  
71 geochronology zircon

72

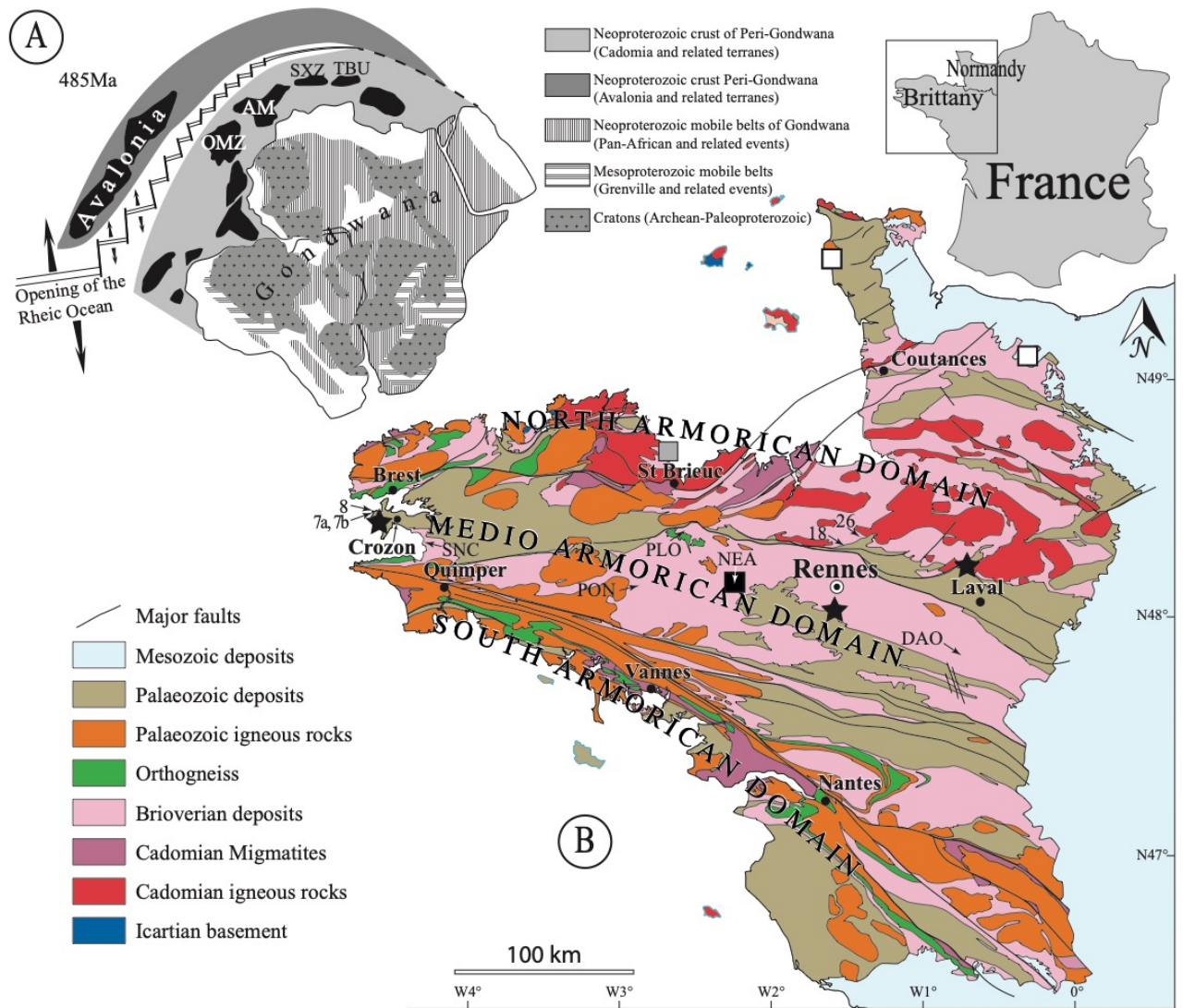
### 73 **1. Introduction**

74

75 The present study aims to analyse the provenance of sediments of the Armorican Massif (West  
76 France), from the Ediacaran-early Cambrian (Cadomian cycle) to the Late Ordovician, and to discuss  
77 the palaeogeographic implications of the results. For this area, palaeogeographic reconstructions have  
78 been established on geodynamic arguments, i.e. evolution of the Cadomian Belt during the Ediacaran  
79 and rifting of the Rheic Ocean in the Cambrian and opening in the Early Ordovician (e.g. Chantaine  
80 et al., 2001; Linnemann et al., 2014). In addition, and especially for the Palaeozoic times, stratigraphic  
81 and palaeontological arguments have been used, e.g., the strong affinities between benthic fauna of  
82 the Medio and North Armorican Domain (Armorican Massif) and the Central Iberian Zone (Iberian  
83 Massif) (Paris and Robardet, 1977; Young, 1988; Robardet, 2002). These arguments have suggested  
84 geological continuity between the Armorican Massif and the Iberian and Bohemian massifs, and  
85 allowed to locate the Armorican Massif at the periphery of the Gondwana supercontinent, close to  
86 the West African Craton and Trans-Saharan Belt (e.g., Linnemann et al., 2008; Avigad et al., 2012;

87 Pereira et al., 2012a, b). However, these proxies are not homogeneous, and they do involve very large  
88 areas. This is the case with some stratigraphic evolutions that may be controlled by allocyclic factors  
89 (e.g., sea level variations) or with faunal assemblages that have a wide provincial distribution and  
90 appear rather homogeneous over vast domains. To reconstruct the palaeogeographic position, other  
91 approaches can be used such as the characterization of source areas of siliciclastic supplies. In  
92 particular, detrital zircon age dating is a powerful tool to analyse the provenance of clastic sediments  
93 and to discuss palaeogeography and tectonic evolution of continental realms. Only few detrital zircon  
94 data are available for the Armorican Massif (i.e. Fernández-Suráez et al., 2002a; Strachan et al., 2014;  
95 Gougeon et al., 2018; Ballouard et al. 2018) but there is an abundant chronological literature  
96 concerning the Iberian Massif (e.g., Fernández-Suárez et al., 2000, 2002b; Pereira et al., 2012a, b;  
97 Shaw et al., 2014; Talavera et al., 2015), Saxo-Thuringia (Linnemann et al., 2008) and North Africa  
98 (e.g., Meinhold et al., 2011; Avigad et al., 2012; Gärtner et al., 2016).

99 The purpose of the present study is to identify the origin of Ediacaran to Upper Ordovician  
100 sediments in the Crozon Peninsula within the Medio Armorican Domain (Fig. 1), with the application  
101 of U-Pb LA-MC-ICP-MS geochronology on detrital zircons coupled with whole-rock Sm-Nd and  
102 Lu-Hf on zircon isotope analyses. As a consequence, the affinity between the Iberian and Armorican  
103 massifs will be considered in order to discuss the palaeogeographic location of the Medio Armorican  
104 Domain at the North Gondwana margin and its relations with the Iberian Massif.



105

106 Fig. 1: (A) Schematic palaeogeographical reconstruction of the Gondwana supercontinent around 485  
 107 Ma (modified from Linnemann et al., 2008). In black are still recognisable terranes OMZ: Ossa  
 108 Morena Zone; AM: Armorican Massif; SXZ: Saxo-Thuringian Zone; TBU: Tepla-Barrandian Unit.  
 109 (B) Simplified geological map of the Armorican Massif modified after Chantraine et al. (1996) and  
 110 location of the studied samples in the Medio Armorican Domain (black stars). Samples from  
 111 Normandy (white squares: Strachan et al., 2014), North Brittany (grey square: Fernández-Suárez et  
 112 al., 2002a), Central Brittany (black square; Gougeon et al., 2018), samples NEA, PON, DAO, PLO,  
 113 SNC from Dabard et al. (1996) and samples 7a, 7b, 8, 18 and 26 from Michard et al. (1985).  
 114

115

## 116 2. Geological setting

117

118 Late Carboniferous transcurrent shear zones (Jégouzo, 1980; Gapais and Le Corre, 1980)  
 119 subdivide the Armorican Massif into three domains, the North Armorican Domain (NAD) and the

120 Medio Armorican Domain (MAD) that are grouped together into the Medio-North Armorican  
121 Domain (MNAD), and the South Armorican Domain (Fig.1). These domains record distinct tectonic  
122 and magmatic evolutions during the Cadomian and Variscan orogenesis.

123 During the Neoproterozoic, the Armorican Massif has experienced a suite of extensive and  
124 compressive episodes associated with magmatism that led to the development of the Cadomian Belt  
125 (cf. synthesis in Chantraine et al., 2001). The main evidence for the Cadomian orogeny, which is a  
126 part of the Pan-African orogeny, derives from the NAD. In North Brittany, geochemical studies (e.g.  
127 Thiéblemont et al., 1999) demonstrated the existence of continental arcs around 750-650 Ma  
128 (Eocadomian) that affected the Icartian basement (1.8 to 2.1 Ga). Subsequently, several episodes of  
129 magmatic activity succeeded each other (ca. 620 - 575 Ma and ca. 555 - 530 Ma). At the same time,  
130 a thick siliciclastic succession, called the Brioverian Supergroup, accumulated in extensional basins.  
131 They are divided into two groups. The lower Brioverian Group of Ediacaran age is located in the  
132 NAD and is made up of sediments containing interbedded graphitic cherts (phtanites: Dabard, 2000)  
133 or devoid of cherts. This group was deposited between 624 Ma, the age of the youngest detrital zircon  
134 grains in the basal part of the group (e.g., Poudingue de Cesson: Samson et al., 2003) and about 580  
135 Ma, the age of plutonic intrusions into the sedimentary successions (e.g., Coutances quartz diorite:  
136 Guerrot and Peucat, 1990; Saint Quay diorite: Nagy et al., 2002). The upper Brioverian Group of late  
137 Ediacaran to early Cambrian age (Guerrot et al., 1992; Gougeon et al., 2018) is present in the three  
138 domains and is composed of sediments containing chert clasts.

139 In the MAD, the upper Brioverian sediments consist of several thousand metre thick alternations  
140 of wackes and siltstones that were mainly deposited in various sedimentary environments ranging  
141 from submarine fans to continental shelf deposits. The latter are represented by distal facies until tidal  
142 plain facies. These sedimentary strata were in part slightly deformed during the Cadomian orogeny  
143 (Le Corre, 1977). The lower Palaeozoic deposits consist mainly of siliciclastic lithofacies alternating  
144 with some carbonate levels (Paris et al., 1999; Vidal et al., 2011a). The sedimentation of the  
145 Brioverian sediments began between the Tremadocian and the Floian (Lower Ordovician) with the

146 Initial Red Beds (Cap de la Chèvre Formation in the Crozon Peninsula) and the Grès Armoricaïn  
147 Formation (Fm), which rest unconformably on the Brioverian strata (Fig. 2). The Initial Red Beds  
148 are characterized by lateral facies variations and were deposited in alluvial to deltaic environments  
149 (Bonjour, 1988; Suire et al., 1991). The Grès Armoricaïn Fm was deposited in wave- and tide-  
150 dominated nearshore environments (Dabard et al., 2007; Pistis et al., 2016). The significant lateral  
151 thickness variations (0 to 100 m for the Initial Red Beds and 20 to 700 m for the Grès Armoricaïn  
152 Fm) are related to the extensional event that led to the progressive opening from west to east, in  
153 present coordinates, of the Rheic Ocean between southern Avalonia and North Gondwana (Fig. 1a).  
154 A model of tilted blocks associated with listric faults was proposed for the Initial Red Beds (Dauteuil  
155 et al., 1987; Brun et al., 1991). For the Grès Armoricaïn Fm, the high thicknesses of several hundreds  
156 of metres in iso-facies are explained by high subsidence rates. The lateral variations of thicknesses  
157 are linked to tectonically-controlled depocenters constantly filled in by oversupplied nearshore  
158 depositional systems (Dabard et al., 2015). From the Darriwilian (Middle Ordovician), the subsidence  
159 rate stabilized around 20 m/my, which is interpreted as post-rift thermal subsidence (Dabard et al.,  
160 2015). Up to the end of the Ordovician, the sediments were laid down in a continental shelf whose  
161 main architecture was controlled by high glacio-eustatic variations under Icehouse conditions  
162 (Dabard et al., 2015). Until the Sandbian (early Late Ordovician), the sedimentation is represented  
163 by silty-clayey lithofacies (Postolonnec Fm on the Crozon Peninsula, 400 m thick, Fig. 2) deposited  
164 in a storm-dominated shelf environment (Dabard et al., 2015). After a major sea-level fall, the  
165 sedimentation continued into the Katian with micaceous sandstones, quartzarenites and mudstones  
166 (Kermeur Fm on the Crozon Peninsula, 90 to 450 m thick, Fig. 2) deposited in bay/lagoon-barrier  
167 environments evolving towards open shelf settings (Vidal et al., 2011b; Gorini et al., 2008). Then  
168 sedimentation continued, without significant interruptions, until the Carboniferous with development  
169 of several thousand metre thick deposits.

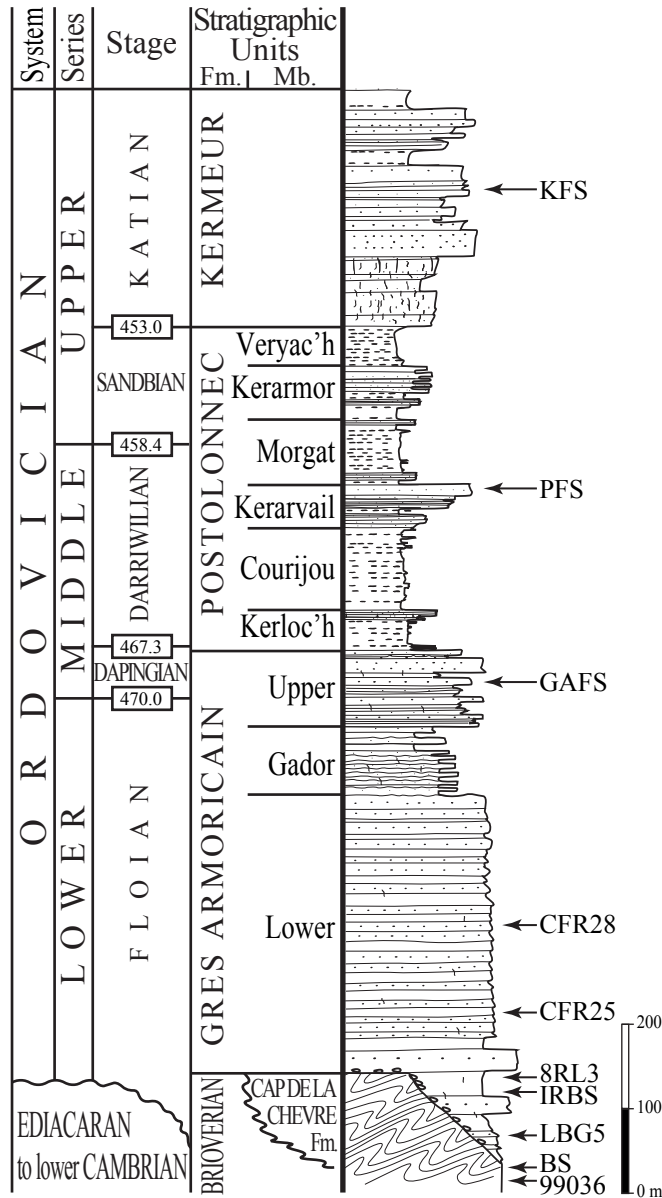
170 The samples for the U-Pb LA-MC-ICP-MS geochronology of detrital zircons were collected on  
171 the Crozon Peninsula (western part of the MAD, Figs. 1 and 2) at Trez Bihan (BS and IRBS samples,

172 at N 48°13'07.16"; W 4°22'57.36" and coordinate: N 48°13'15.70"; W 4°23'56.25", respectively),  
173 Morgat (GAFS sample, N 48°13'18.92"; W 4°29'43.43"), Postolonnec (PFS sample, N 48°14'17.47";  
174 W 4°28'06.24") and Veryarc'h (KFS sample, N 48°15'40.15"; W 4°36'29.19") along beach cliffs. The  
175 Brioverian BS sample is a fine quartz wacke with matrix and was taken about 10 meters below the  
176 post Cadomian angular unconformity surface. The IRBS sample (Cap de la Chèvre Fm) is a subarkose  
177 with abundant lithic fragments, collected about 80 meters above the same angular unconformity. The  
178 IRBS sample (Cap de la Chèvre Fm) is a subarkose with abundant lithic fragments, collected about  
179 80 meters above the angular discordance. The GAFS sample (Grès Armoricain Fm) is a fine-grained  
180 quartz arenite without matrix with abundant heavy minerals (e.g., rutile, zircon, monazite, tourmaline,  
181 ...), collected about 60 meters below the stratigraphic boundary with the overlying Postolonnec Fm.  
182 The PFS sample (Postolonnec Fm) is a medium grained quartz arenite without matrix, taken at 136  
183 meters from the base of the formation. The KFS sample (Kermeur Fm) is a medium grained quartz  
184 arenite with low matrix content, which was collected at 114 meters from the base of the formation.

185 Some Sm-Nd whole-rock data of sedimentary rocks are partly provided from published data (for  
186 details see Michard et al., 1985; Dabard et al., 1996). The samples of this study (Fig 1 and Fig 2)  
187 come from different localities of the MAD. The sample of Brioverian quartz wacke, 99036, was taken  
188 at about 9 km from North Laval (black star in Fig. 1, N 48°09'22.21"; W 0°44'47.92"). The sample  
189 of sandy siltstone from the Initial Red Beds, LBG5-8872, was taken at Pont Réan (South of Rennes,  
190 black star in Fig. 1, at N 47°59'45.99"; W 1°45'00.26"). The quartz wacke sample 8RL3-8881, also  
191 from the Initial Red Beds succession, was taken at Cap de la Chèvre (Crozon Peninsula, black star in  
192 Fig. 1, at N 48°10'14.78"; W 4°32'25.62"). Two samples of very fine quartz arenite from the Grès  
193 Armoricain Fm, denoted CFR25-5618 and CFR28-5617, were taken at the old quarry of Camp  
194 Français in North Laval (black star in Fig. 1, at N 48°09'17.52"; W 0°44'51.47" and N 48°09'18.99";  
195 W 0°44'59.33", respectively). All samples are poor in heavy mineral content and, if any, have a fine  
196 phyllosilicate matrix.

197





199

200 Fig.2: Lithostratigraphic (x-axis represents grain-size from mudstone to conglomerate) context of the  
 201 Lower Palaeozoic succession in the Crozon Peninsula (modified after Vidal et al., 2011a). This figure  
 202 indicates the stratigraphic positions of the studied samples.  
 203

204

205

206 **3. Methodology**

207

208 The Sm and Nd concentrations were obtained by the isotope dilution method, using on a Cameca  
209 TSN 206 mass spectrometer at Rennes University. Total blanks for the chemical separations are  
210 estimated around 0.1 ng for the Nd. Isotopic compositions of the Nd have been determined using a  
211 Finnigan MAT 262 mass spectrometer. Isotopic ratios were normalized to  $^{146}\text{Nd}/^{144}\text{Nd} = 0.7219$ . The  
212 results are reported to the La Jolla Nd standard (= 0.511860). The detailed technique on Sm-Nd is  
213 reported in Jahn et al. (1980). Precisions of the measurements are given at the 95% confidence level.  
214  $T_{\text{DM}}$  model ages were calculated according to DePaolo (1981).

215 Zircon concentrates were extracted from 3-4 kg of each rock sample first by crushing and then  
216 using conventional magnetic and heavy liquid separation techniques. The samples were not sieved  
217 before zircon separation. For each sample, an arbitrary aliquot of this detrital zircon fraction, almost  
218 150 zircon grains per sample, were put in a glass with ethanol and picked randomly with a pipette  
219 under a binocular microscope, without introducing any bias. This technique avoids any bias because  
220 the grains are randomly selected without any pre-consideration of size, color or shape (Sláma and  
221 Košler, 2012). Afterwards, the zircon grains were mounted into epoxy blocks, and polished to about  
222 half thickness in order to better expose internal surfaces. Then, the blocks were sputtered with carbon  
223 and zircon were examined for internal structures (such as magmatic zonation or metamorphic rims)  
224 using the FEI Quanta 450 scanning electron microscopy at the University of Brasilia.

225 The U–Pb and Lu–Hf isotopic analyses were performed on zircon using a Thermo-Fisher Neptune  
226 MC-ICP-MS coupled with a Nd:YAG UP213 NewWave laser ablation system (Laboratory  
227 Conditions in Supplementary Materials), installed in the Laboratory of Geochronology and Isotope  
228 Geochemistry of the Brasilia University.

229 The U-Pb analyses on zircon grains were carried out using the standard-sample bracketing method  
230 (Albarède et al., 2004) using the GJ-1 (Jackson et al., 2004) as first standard zircon in order to quantify  
231 the amount of ICP-MS fractionation. Between four and eight (when little fractionation is observed)  
232 unknown zircon samples were analysed between each two GJ-1 reference material analyses  
233  $^{206}\text{Pb}/^{207}\text{Pb}$  and  $^{206}\text{Pb}/^{238}\text{U}$  ratios have been time corrected. The raw data were processed off-line and

234 reduced using an Excel worksheet (Bühn et al., 2009). Analyses were performed using generally a  
235 spot size of 30  $\mu\text{m}$ , and laser induced fractionation of the  $^{206}\text{Pb}/^{238}\text{U}$  ratio was corrected using the  
236 linear regression method (Koşler et al., 2002). During each analytical session, the zircon standard  
237 Temora-2 (Black et al., 2004; Temora U/Pb data in Supplementary Material), for which the  
238 recommended age is 390-420 Ma, was also analysed as a secondary zircon standard.

239 Lu–Hf isotopes were analysed in selected zircon grains previously analysed with the U–Pb  
240 method. The selection was made on the basis of highest concordance values (95-105%) and for  
241 representativity of all observed U-Pb age groups in a sample’s age population. Lu–Hf isotopic  
242 analyses were performed following the methodology of Matteini et al. (2010). The  $\epsilon_{\text{Hf}}(t)$  values were  
243 calculated using the decay constant  $\lambda = 1.865 \cdot 10^{-11} \text{ yr}^{-1}$  proposed by Scherer et al. (2001) and the  
244  $^{176}\text{Lu}/^{177}\text{Hf}$  and  $^{176}\text{Hf}/^{177}\text{Hf}$  CHUR values of 0.0336 and 0.282785 (Bouvier et al., 2008). A two-stage  
245  $T_{\text{DM}}$  age was calculated from the initial Hf isotopic composition of the zircon, using an average crustal  
246 Lu/Hf ratio of 0.0113 (Gerdes and Zeh, 2006, 2009, Nebel et al., 2007). This value was selected  
247 because it represents best the composition of a hypothetical crust. The initial Hf composition of zircon  
248 represents the  $^{176}\text{Hf}/^{177}\text{Hf}$  value calculated at the time of zircon crystallization, given by the U-Pb age  
249 previously obtained on the same grain and that, if possible, should be concordant. The two-stage  
250 depleted mantle Hf model ages ( $T_{\text{DM}} \text{ Hf}$ ) are calculated using  $^{176}\text{Lu}/^{177}\text{Hf}=0.0384$  and  
251  $^{176}\text{Hf}/^{177}\text{Hf}=0.28325$  for the depleted mantle (Chauvel and Blichert-Toft, 2001) and a  $^{176}\text{Lu}/^{177}\text{Hf}$   
252 value of 0.0113 for average crust (Taylor and McLennan, 1985 / Wedepohl, 1995).

253 Before Hf isotope measurements on zircons, replicate analyses of a 200 ppb Hf JMC 475 standard  
254 solution doped with Yb (Yb/Hf=0.02) were carried out with this result:  $^{176}\text{Hf}/^{177}\text{Hf}=0.282162 \pm 13$ , 2s  
255 error,  $n=4$ . During the analytical session replicate analyses of the GJ-1 standard zircon were made,  
256 which gave an average  $^{176}\text{Hf}/^{177}\text{Hf}$  ratio of  $0.282006 \pm 16$  2s ( $n=25$ ), in agreement with the reference  
257 value for the GJ standard zircon (Morel et al., 2008).

258

#### 259 **4. Analytical results**

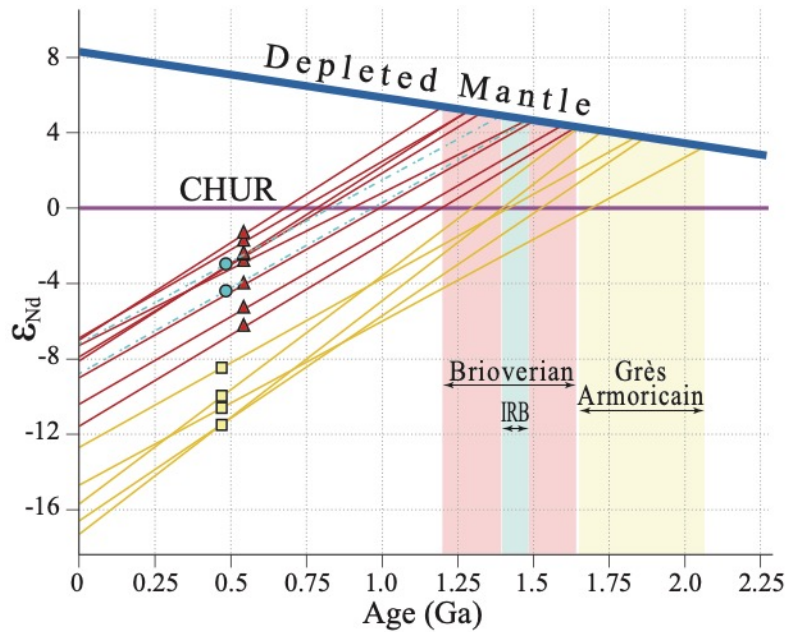
260 4.1. Whole rock Sm-Nd isotopic analyses

261 The  $^{143}\text{Nd}/^{144}\text{Nd}$  initial ratios and  $\epsilon_{\text{Nd}}$  were recalculated for each formation, taking into  
 262 account the stratigraphic available age. Samples from the upper Brioverian Group yield negative  $\epsilon_{\text{Nd}}$   
 263 (540) values between -1.4 and -6.3 (Tab. 1, Fig. 3) and Mesoproterozoic Nd model ages ranging  
 264 between 1.2 and 1.6 Ga, respectively. The two IRB samples have also negative  $\epsilon_{\text{Nd}}$  (480) values of -  
 265 3.0 and -4.4 and Mesoproterozoic Nd model ages of 1.4 and 1.5 Ga, similar with the obtained data  
 266 for the Brioverian sediments. For the Grès Armoricaïn Fm, all analyzed samples exhibit much  
 267 negative  $\epsilon_{\text{Nd}}$ (470) values between -8.5 and -11.5 and Paleoproterozoic Nd model ages ranging from  
 268 1.7 to 2.1 Ga, respectively.

269

samples	Ages Ma	Sm	Nd	$^{147}\text{Sm}/^{144}\text{Nd}$	$^{143}\text{Nd}/^{144}\text{Nd}$ ( $\pm 2\sigma$ )	$\epsilon_{\text{Nd}(0)}$	$\epsilon_{\text{Nd}(t)}$	$T_{\text{DM}}$ (Ga)
<b>Brioverian</b>	<b>540</b>							
NEA (1)		2.96	15.36	0.1164	0.512283(6)	-7.0	-1.4	1.20
PON (1)		5.89	29.04	0.1225	0.512285(5)	-6.9	-1.8	1.28
DAO (1)		3.09	15.64	0.1194	0.512045(6)	-11.6	-6.3	1.64
PLO (1)		2.81	13.95	0.1219	0.512100(7)	-10.5	-5.4	1.60
SNC (1)		4.34	22.62	0.116	0.512227(5)	-8.1	-2.5	1.28
8 (2)		5.95	27.2	0.1323	0.512266(28)	-7.3	-2.9	1.48
26 (2)		8.33	39.91	0.1263	0.512180(34)	-9.0	-4.1	1.50
99036 (3)		4.81	24.19	0.1201	0.512237(5)	-7.9	-2.6	1.33
<b>Initial Red Beds</b>	<b>480</b>							
LBG5-8872 (3)		6.07	29.28	0.1254	0.512191(3)	-8.8	-4.4	1.48
8RL3-8881 (3)		2.58	12.26	0.127	0.512269(3)	-7.2	-3.0	1.39
<b>Grès Armoricaïn Fm</b>	<b>470</b>							
7b (2)		9.57	45.99	0.1259	0.511988(29)	-12.7	-8.5	1.84
7a (2)		1.85	10.09	0.1109	0.511788(35)	-16.6	-11.5	1.87
18 (2)		3.76	22.43	0.1014	0.511755(33)	-17.3	-11.5	1.73
CFR25-5618 (3)		7.56	44.65	0.1023	0.511837(3)	-15.7	-10.0	1.65
CFR28-5617 (3)		18.13	85.24	0.1285	0.511885(3)	-14.7	-10.6	2.07

270 Table 1: Whole rock Sm and Nd concentrations and Nd isotope data of Brioverian and Lower Ordovician sedimentary  
 271 rocks. Data (1) from Dabard et al. (1996), (2) Michard et al. (1985) and (3) this work (LBG5: Pont Réan, South of  
 272 Rennes; 8RL3: Crozon Peninsula; 99036, CFR25 and CFR28: North Laval).  $T_{\text{DM}}$  model ages calculated  
 273 according to DePaolo (1981).  
 274  
 275



276

277 Fig.3: Age (Ga) versus  $\epsilon_{Nd(t)}$  diagram for the Brioverian (red triangles), Initial Red Beds (IRB) (blue  
 278 circles) and Grès Armoricain (yellow squares) samples.

279

280

281

#### 4.2. Detrital zircon ages

282

283

284

285

286

287

288

Generally, the sizes of the zircon grains of the analysed samples are not larger than 260  $\mu\text{m}$  and the most frequent size is around 100  $\mu\text{m}$ . The zircon grains of the GAFS (Grès Armoricain Fm) sample are very well sorted and, on average, smaller than those of the other samples. The zircon grains are generally colourless or weakly coloured and have euhedral shapes with rare rounded grains. An exception is the GAFS sample and, to a minor degree, the samples from overlying strata, where many coloured and rounded grains are observed that testify to long transport processes or multiple deposition/alteration/transport cycles.

289

290

291

292

293

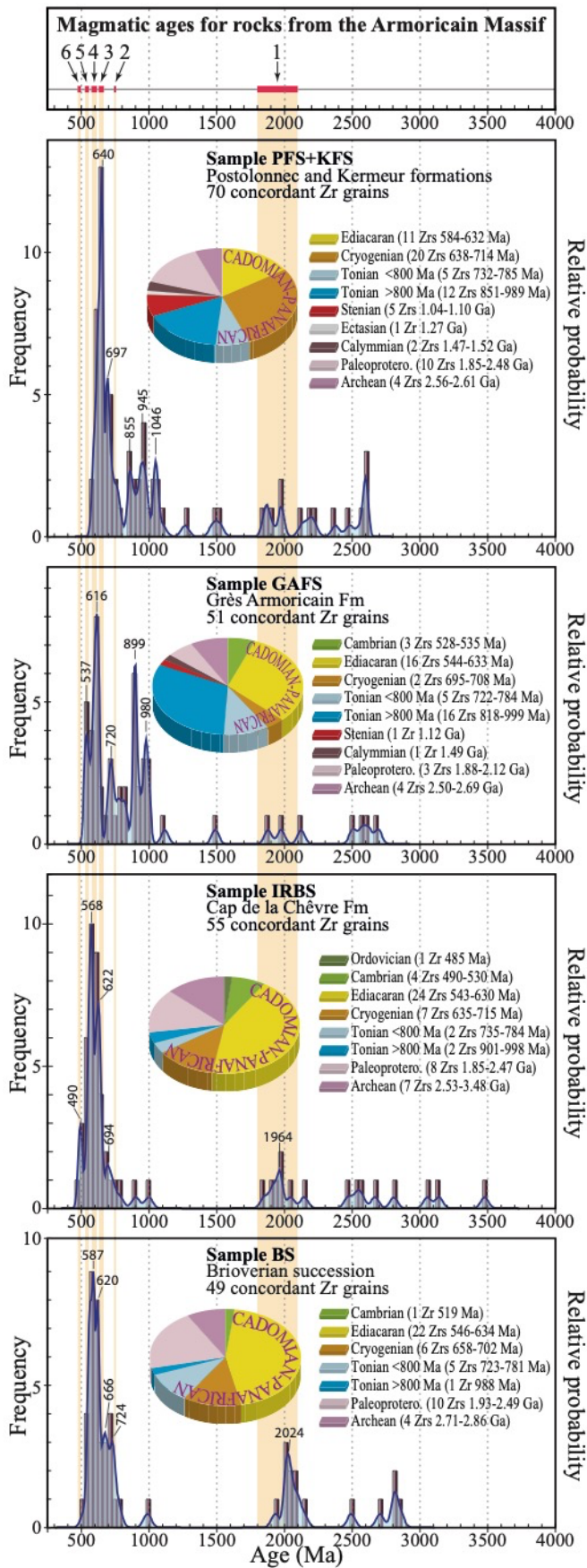
From the Brioverian sample (BS) 68 detrital zircon grains were analysed and 49 gave concordant data (Fig. 4 and U/Pb data in Supplementary Material). The most abundant age population (67%) is Ediacaran to Tonian, <800 Ma, in age (33 zircon grains). The Kernel probability plot shows two Ediacaran major peaks (587 Ma and 620 Ma) and two minor Cryogenian (666 Ma) and Tonian (724 Ma) peaks. There is a prominent age gap between 781 Ma and 1.93 Ga (Orosirian) with the exception

294 of a single zircon grain of 988 Ma age. Ten zircon grains yielded Paleoproterozoic ages, giving a  
295 peak at 2.02 Ga, and four grains yielded Archean ages.

296 In the Lower Ordovician sample (IRBS), 55 detrital zircon grains gave concordant results, out of  
297 69 analysed grains. The ages for most abundant zircon population (38 zircon grains) gave ages from  
298 Furongian (latest Cambrian) to Tonian <800 Ma, with 24 zircon grains being Ediacaran in age. The  
299 Kernel probability plot shows two Ediacaran major peaks (568 Ma and 622 Ma) and two minor peaks  
300 at 490 Ma (late Cambrian) and 694 Ma (Cryogenian). There is a prominent age gap between the  
301 Tonian <800 Ma and the Orosirian, with exception of two zircon grains with ages of 901 and 998  
302 Ma. The other zircon grains are Paleoproterozoic (8 zircon grains, minor peak at 1.96 Ga) and  
303 Archean (7 zircon grains, 2.53 – 3.48 Ga) in age.

304 In the Floian sample (GAFS) 51 zircon grains are concordant (69 analysed grains). The Kernel  
305 plot shows numerous age peaks between the Cambrian and Stenian with major peaks located at 537,  
306 616, 720, 899, and 980 Ma. Abundant grains have Ediacaran and Tonian ages are abundant (16 and  
307 19 zircon grains, respectively), whilst only one grain yielded a Stenian age . The youngest concordant  
308 zircon grains are Fortunian in age (528-535 Ma), and the oldest data are Paleoproterozoic and  
309 Neoproterozoic, with ages between 1.88 and 2.69 Ga.

310 The PFS+KFS sample combines two samples from the Postolonnec (PFS) and the Kermeur (KFS)  
311 formations (Middle and Upper Ordovician, respectively). Seventy zircon grains are concordant, out  
312 of an analysed population of 134 grains. The Kernel probability plot shows two main populations: an  
313 Ediacaran to Tonian <800 Ma one with 584 to 785 Ma ages for 36 zircon grains and major peaks at  
314 640 and 697 Ma; and another of Tonian (>800 Ma) to Stenian age, with several minor peaks at 855,  
315 945 Ma, and up to 1.05 Ga (17 zircon grains). The age distribution shows a gap at 800 Ma in the age  
316 diagram between these two age populations. The ages of the other zircon grains are widely dispersed  
317 over the Calymmian (early Mesoproterozoic), Orosirian (Paleoproterozoic), and Neoproterozoic.



318  
319  
320  
321

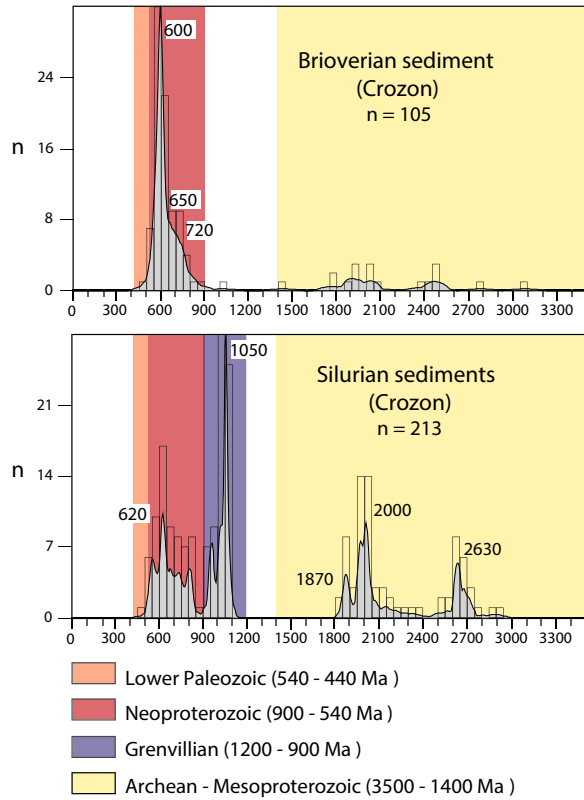
Fig.4: U-Pb ages of detrital zircon grains from the studied samples: frequency and Kernel density estimate (KDE) distribution plots. The  $^{207}\text{Pb}/^{206}\text{Pb}$  and the  $^{206}\text{Pb}/^{238}\text{U}$  ages have been used for zircon grains older and younger than 1 Ga, respectively. The vertical orange bands shown in the figure

322 represent the main range ages for magmatic rocks. Magmatic rock ages are from (1) Auvray et al.  
323 (1980), Inglis et al. (2004), Samson and D'Lemos (1998), Vidal (1980), Martin et al. (2018); (2)  
324 Samson et al. (2003), Egal et al. (1996); (3) Samson et al. (2003), Guerrot and Peucat (1990), Graviou  
325 et al. (1988), Nagy et al. (2002); (4) Vidal (1980), Chantraine et al. (1999, 2001), Egal et al. (1996),  
326 Inglis et al. (2005), Cocherie et al. (2001), Guerrot and Peucat (1990), Peucat et al. (1981), Vidal et  
327 al. (1974), Strachan et al. (1996), Miller et al. (2001), Cocherie et al., 2001; (5) Auvray (1979),  
328 Graviou et al. (1988), Egal et al. (1996), Guerrot et al. (1992), Pasteel and Doré (1982), Peucat (1986),  
329 Chantraine et al. (2001), Hebert et al. (1993), Guerrot and Peucat (1990), Marcoux et al. (2009); (6),  
330 Guerrot et al. (1992), Auvray et al. (1980), Bonjour et al. (1988), Miller et al. (2001), Ballouard et al.  
331 (2018).

332  
333  
334 As the total number of studied zircon grains with concordant ages per sample is low, comparison  
335 with data from a recent compilation made for the same locations of this study (Ballouard et al., 2018)  
336 is made. This allows to make up for the loss of underrepresented zircon age populations (Fig. 5). In  
337 this work, a Brioverian and a Silurian sample from the Crozon Peninsula in the Medio Armorican  
338 Domain have been analyzed. For our Brioverian sample, the probability curve (BS in Fig. 4.) and the  
339 sample studied by Ballouard et al. (2018) in Fig. 5 are very similar. For the Ordovician samples it is  
340 not possible to make a direct comparison, as these materials are not represented in the work by  
341 Ballouard et al. (2018). Nevertheless it is possible to observe a coincidence of our data with the main  
342 populations of the Silurian sample from Crozon (213 zircons analyzed), in which the gap in the age  
343 diagram that separates the two main age populations for the lower Cambrian to Tonian <800 Ma and  
344 the for Tonian >800 Ma to Stenian ages, is also evident.

345





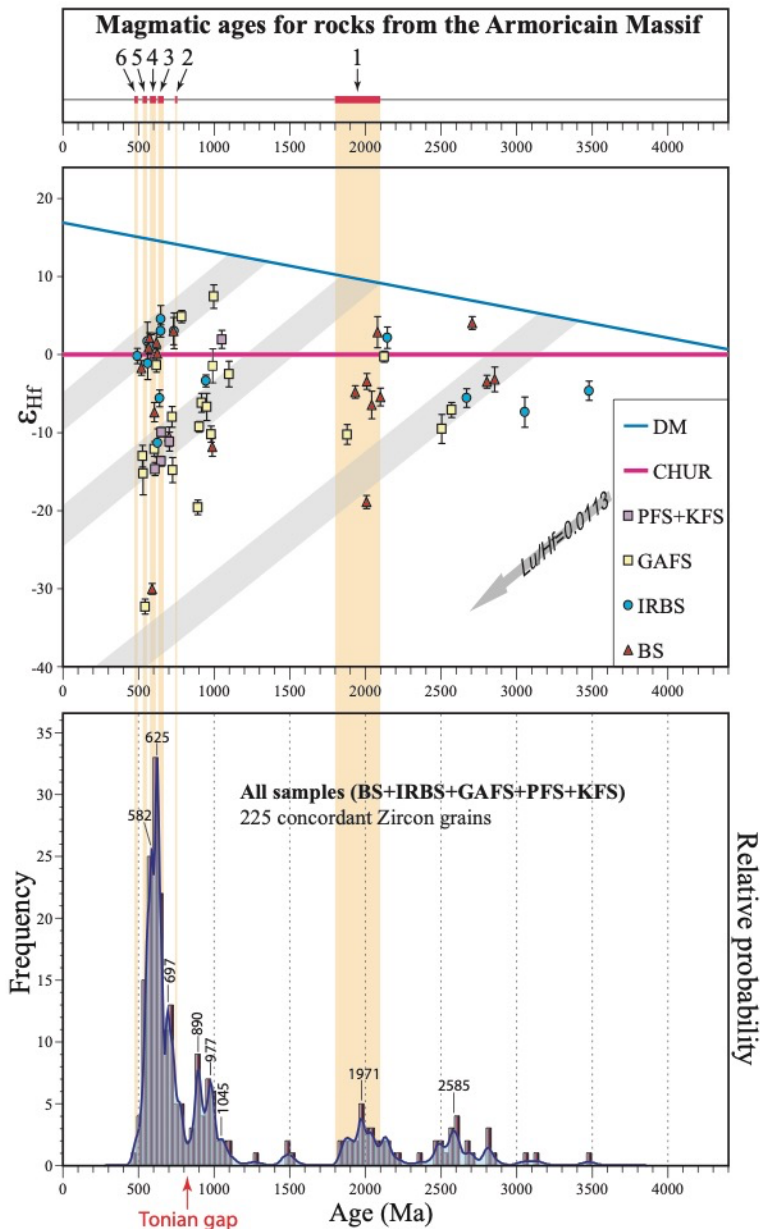
346

347 Fig. 5: U-Pb ages of detrital zircon grains for samples from the Crozon Peninsula (Medio Armorican  
 348 Domain). Histogram and Kernel Density Estimate (KDE) modified after Ballouard et al. (2018).  
 349

350

351 4.3. Lu-Hf on detrital zircons

352 In order to characterize by Lu-Hf isotope the recognized zircon populations with Lu-Hf isotope ratios,  
 353 nineteen zircons of the main populations were selected from the Brioverian (BS) (Lu/Hf data in the  
 354 Supplementary Materials). The results show variable  $\epsilon_{\text{Hf}(t)}$  values ranging from -30 to +4, suggesting  
 355 the involvement of Ediacaran-Cryogenian magma and Paleoproterozoic juvenile input (at 2.1 and 2.7  
 356 Ga).



357

358 Fig. 6: U/Pb Age (Ga) versus  $\epsilon_{\text{Hf}}$  for selected zircon grains from this study. DM indicates Depleted  
 359 Mantle and CHUR is Chondritic Uniform Reservoir; Grey domains represents the  $\epsilon_{\text{Hf}(t)}$  bulk-rock  
 360 evolution trends for terranes of different ages that could be recognized by the studied samples,  
 361 calculated using  $^{176}\text{Lu}/^{177}\text{Hf}$  of 0.0113 (Taylor and McLennan, 1985; Wedepohl, 1995). Numbers  
 362 indicate magmatic ages, whose references are listed in Fig. 4 caption.  
 363

364 The fourteen representative zircons from the Lower Ordovician sample (IRBS) vary in  $\epsilon_{\text{Hf}(t)}$  values  
 365 from -11 to +4, suggesting both the supply of juvenile material mainly in the Cryogenian, and  
 366 reworking of the older pre-existing crust.

367 Twenty representative zircon crystals from the Ordovician (Floian) sample (GAFS) gave  $\epsilon_{\text{Hf}(t)}$  values  
368 between -32 and +7, which indicates a juvenile contribution for the zircon grains of Tonian age, and  
369 for the remaining grains recycling of the oldest Paleoproterozoic and Archean crust.

370 The five representative zircon crystals of sample PFS+KFS gave  $\epsilon_{\text{Hf}(t)}$  values ranging from -14 to +3,  
371 suggesting a juvenile contribution for the Stenian zircons and reworking of Paleoproterozoic crust for  
372 the Cryogenian population.

373 The Hf data obtained allow to draw the following magmatic chronological evolution:

374 - The Archean population involves zircon grains from the Neoarchean and Mesoarchean. The  
375 Neoarchean population, represented by zircon grains from the BS, IRBS, and GAFS samples, shows  
376 negative and positive  $\epsilon_{\text{Hf}(t)}$  values (between -9.52 and +4.04). The  $T_{\text{DM}}$  model ages indicate reworking  
377 of Paleoarchean (3.5 Ga) to Mesoarchean crust (2.92 Ga). The Mesoarchean population, represented  
378 by zircon grains from the BS and IRBS samples, show negative  $\epsilon_{\text{Hf}(t)}$  values between -7.37 and -3.18.

379 The  $T_{\text{DM}}$  model ages indicate reworking of Eoarchean (3.84 Ga) to Paleoarchean crusts (3.44 Ga).

380 - Paleoproterozoic magma input provided zircon grains from the Rhyacian and Orosirian periods. The  
381 Rhyacian population from the BS, IRBS, and GAFS samples gave negative to positive  $\epsilon_{\text{Hf}(t)}$  values  
382 between -5.44 and + 2.88, with a  $T_{\text{DM}}$  indicating reworking of Mesoarchean (2.95 Ga) to Siderian  
383 (2.47 Ga) crust. The Orosirian population, represented by zircons from BS and GAFS yielded  
384 negative  $\epsilon_{\text{Hf}(t)}$  values between -18.89 and -3.44, and the  $T_{\text{DM}}$  values of Orosirian zircon indicate  
385 reworking of Eoarchean (3.61 Ga) and Mesoarchean (2.76 Ga) crusts.

386 - A Mesoproterozoic population is only present in the PFS+KFS and GAFS samples. The analysed  
387 zircon crystals from the PFS+KFS sample gave a positive  $\epsilon_{\text{Hf}(t)}$  value of  $\sim +3.0$  and  $T_{\text{DM}}$  model ages  
388 of 1.66 Ga. This suggests reworking of Mesoproterozoic crust. The Stenian zircon in the GAFS

389 sample are characterized by a negative  $\epsilon_{\text{Hf}(t)}$  value of -2.5 and a  $T_{\text{DM}}$  of 1.97, which suggests  
390 reworking of Orosirian crust.  
391 - Neoproterozoic input is evidenced for all the studied samples (37 zircon grains analysed). The  
392 Cryogenian-Ediacarian is represented by zircon grains from the BS, IRBS, GAFS and PFS+KPS  
393 samples. The cryogenian zircon grains have negative to positive  $\epsilon_{\text{Hf}(t)}$  values (-10.52 to +4.57), which  
394 indicates that Rhyacian (2.20 Ga) to Stenian (1.20 Ga) crust was involved. The Tonian population  
395 (which is only missing from the zircon population of the PFS+KFS sample) gave mainly negative  
396  $\epsilon_{\text{Hf}(t)}$  values and indicates that Palaeo- and Mesoproterozoic crust was involved in the generation of  
397 these zircon grains. Only one Neoproterozoic zircon (2.72 Ga) was observed. The Ediacaran zircon grains  
398 with highly negative to slightly positive  $\epsilon_{\text{Hf}(t)}$  values (varying from -32.31 to +2.13) have a  $T_{\text{DM}}$   
399 indicating reworking of Mesoarchean (3.12 Ga) to Ectasian (1.27 Ga) crust.  
400 - Finally, the selected Cambrian to Ordovician zircons displayed negative  $\epsilon_{\text{Hf}(t)}$  values of -1.70 and -  
401 0.18, showing that Mesoproterozoic crust was involved in the recycling.

402

403

## 404 **5. Discussion**

405

### 406 **5.1. General remarks**

407

408 Although the number of zircon grains per sample analysed in this study is lower than desirable, the  
409 reliability of the presented results is verified by the comparison of provenance data compiled recently  
410 by Ballouard et al. (2018). They analyzed a comparatively larger number of zircon grains but obtained  
411 a very similar distribution of population ages (Fig. 5) and also documented the Tonian gap in the data.

412 These data would appear to be indicative of age gaps, but a more robust dataset may eventually  
413 clarify.

414 The sedimentary zircon grains from the Brioverian sample (BS) are mainly of local origin, as deduced  
415 from the perfect coincidence of provenance ages with those of magmatic rocks outcropping in the  
416 Armorican Massif (denoted 1- 6 in Figures 4 and 5). The Lu-Hf isotopic data for the other Ordovician  
417 samples analysed here show zircon grains with different ages but also similar to the ages of the locally  
418 occurring magmatic rocks. However, the  $\epsilon_{\text{Hf}(t)}$  values obtained from the zircon grains of the BS and  
419 IRBS samples, which have an Armorican source area, are mostly positive, whereas the younger  
420 samples (GAFS and PFS+KFS) yielded, on average, negative values (Fig. 6).

421 A comparison of  $\epsilon_{\text{Hf}(t)}$  values from zircon in Cadomian (BS) and post-Cadomian (IRBS, GAFS and  
422 PFS+KFS) samples shows a progressive increase of the proportion of negative values zircon grains  
423 in the post-Cadomian samples the younger the sample, the more abundant the negative values zircon  
424 fraction. This progression is less evident in the IRBS sample, which contains local Cadomian  
425 contributions (pre-Rift deposits), whereas the more recent samples (GAFS and PFS+KFS) show this  
426 trend strongly (in-Rift and post-Rift deposits). This suggests a gradual involvement of other source  
427 areas in the sediment flux that became added to the earlier Cadomian sources.

428 This observation is in agreement with the results obtained by whole-rock Sm-Nd isotopic analysis  
429 (Fig. 3). In particular, the Tonian >800Ma and Stenian populations gave mostly negative  $\epsilon_{\text{Hf}(t)}$  values  
430 that indicate the recycling of an older Orosirian crust (Fig. 6). It should be noted that no zircon from  
431 the Brioverian sample (BS) showed evidence for recycling of Orosirian crust.

432 Furthermore, the U-Pb and Hf isotope results on zircon grains from the Armorican Massif suggest  
433 the importance of recycling of older crust – which is characteristic for the majority of the analysed  
434 samples.

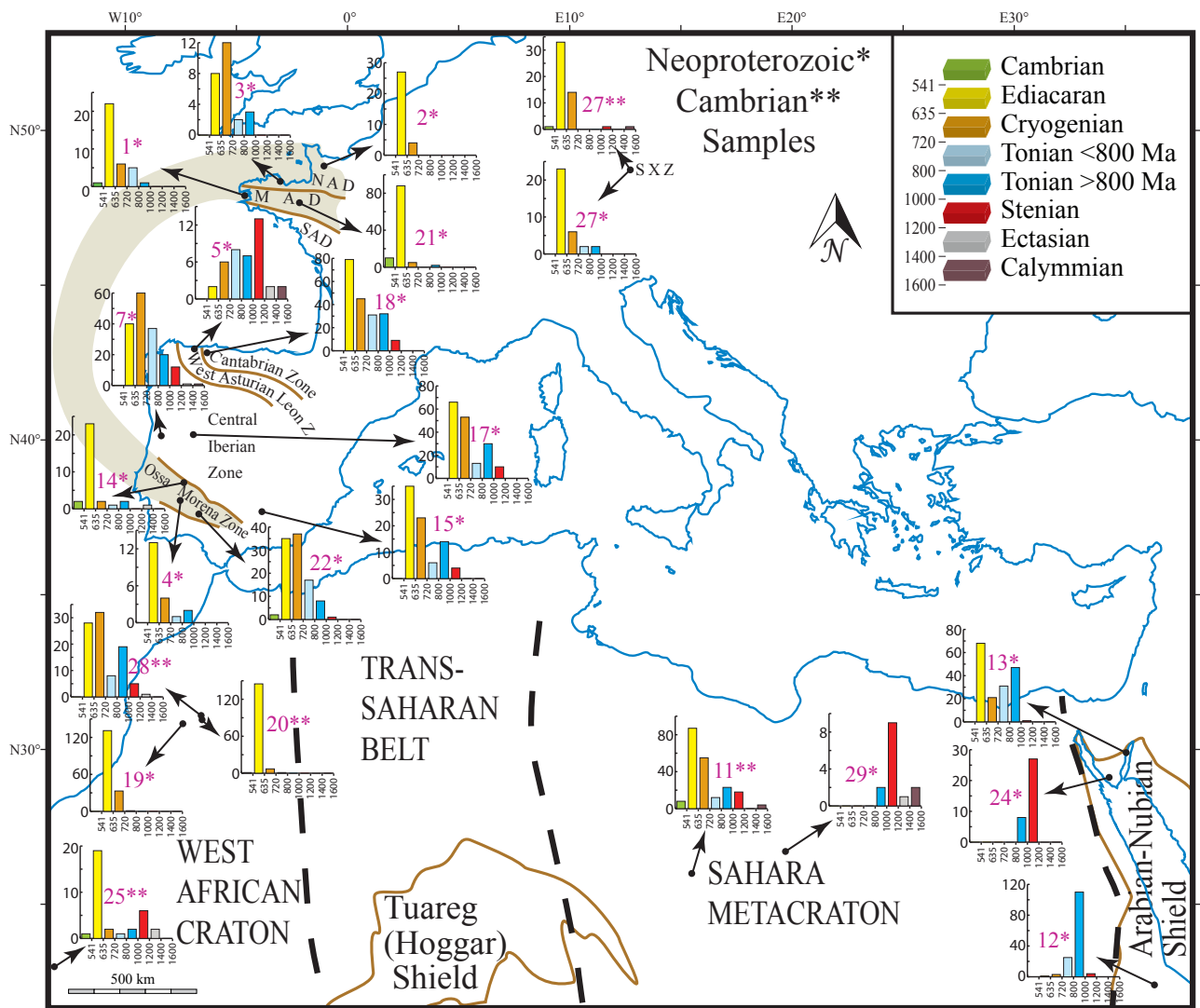
435

436

437 5.2. Upper Brioverian and Cap de la Chèvre Fm

438 The zircon populations of the Brioverian sample (BS) from West Brittany (this study, 1 in Fig. 7)  
439 and others from other Armorican areas (Fig. 7), i.e. Central Brittany (21: Gougeon et al., 2018) and  
440 North Brittany (3: Fernández-Suárez et al., 2002a) and Normady (Samson et al., 2005; 2: Strachan et  
441 al., 2014), show strong similarities: prevalence of Neoproterozoic zircon grains, especially of  
442 Ediacaran and Cryogenian ages, and lack of Mesoproterozoic ones. The main differences between  
443 samples are the total lack of Tonian zircon grains in Normandy and Central Brittany, and for this  
444 latter region, the lack of Paleoproterozoic and Archean zircon grains and the occurrence of Cambrian  
445 zircon grains. Also, in the Brioverian (BS) sample there is a younger age of 519 Ma that may suggest  
446 the possibility of an extension of the Brioverian age until the early Cambrian. This possibility cannot  
447 be ruled out but must be confirmed further, as it has only been detected on a single zircon grain.

448 In the palaeogeographic and orogenic contexts of the Armorican Massif, the potential source areas  
449 for the Brioverian sediments include the Cadomian and Pan-African orogenic belts. The Tonian <800  
450 Ma to Ediacaran ages are consistent with the age of the Cadomian magmatism in the Armorican  
451 Massif, from the Eocadomian (750 - 650 Ma: 2 and 3 in Fig. 4; e.g., Port Morvan orthogneiss,  
452 boulders in Cesson conglomerate: Guerrot and Peucat, 1990; Egal et al., 1996; Samson et al., 2003)  
453 and Cadomian (620 - 575 Ma; 4 in Fig. 4; e.g., North Trégor Batholith, Lanvollon, Erquy, Lézardrieu  
454 and Paimpol formations: Graviou et al., 1988; Egal et al., 1996; Chantraine et al., 1999; Chantraine  
455 et al., 2001; Cocherie et al., 2001; Nagy et al., 2002) episodes, right up to the crustal melting phase  
456 around 540 Ma (5 in Fig. 4; e.g. Mancellian Batholith, Vires and Carolles granites: Graviou et al.,  
457 1988; Pasteel and Doré, 1982). The Paleoproterozoic ages are consistent with the ages found for the  
458 Icartian orthogneissic basement in the region (1 in Fig. 4; e.g., Port Béni, Trébeurden and La Hague  
459 orthogneiss: Auvray et al., 1980; Inglis et al., 2004; Martin et al., 2018). Archean rocks have not been  
460 documented in the Armorican Massif but they could represent the paragneisses associated with the  
461 Icartian complex (e.g. Trébeurden micaschist: Auvray et al., 1980).



462

463 Fig. 7: Map with detrital zircon age spectra for Neoproterozoic (\*) and Cambrian (\*\*) samples. Zircon  
 464 age population diagrams are limited to the sectors with the most significant ages, and the oldest  
 465 Mesoproterozoic ages have been excluded (1600 Ma). Age spectrum 1 (upper left) represents the  
 466 present work (Fig. 4), whereas the other diagrams are extracted from the literature, as mentioned in  
 467 the text.

468

469 Detrital zircon ages in the upper Brioverian sediments of the Medio Armorian Domain (MAD)  
 470 suggest source areas mainly located in the North Armorian Cadomian Belt, although a Gondwana  
 471 source contribution cannot be completely excluded, especially for the Archean zircon population.  
 472 This hypothesis, already suggested by Denis and Dabard (1988) and Dabard (1990), is in agreement  
 473 with the maturity increase of sediments southward in the Medio-North Armorian Domain (MNAD)  
 474 (Chantraine et al., 1983; Denis and Dabard, 1988), and with the occurrence of chert fragments  
 475 providing from the lower Brioverian Group of the North Armorian Domain (NAD). The MAD, thus,

476 could constitute the retro-arc basin of the Cadomian Belt that was mainly fed by its own erosion  
477 products.

478 A comparison with the Iberian Massif (Fig. 7) shows that the zircon grain distribution in the MAD  
479 presents similarities with that observed for samples from the Ossa Morena Zone, with a low  
480 abundance of Tonian >800 Ma ages and the lack of Stenian ages (4: Fernández-Suárez et al., 2002a;  
481 14: Linnemann et al., 2008; 22: Pereira et al., 2012b). In contrast, in the Central Iberian, West  
482 Asturian and Cantabrian zones these populations are significantly present (5: Fernández-Suárez et al.,  
483 2000; 7: Pereira et al., 2012a; 17, 18 : Fernández-Suárez et al., 2014; 15: Talavera et al., 2015).

484 The detrital zircon age population for the Lower Ordovician sample IRBS (Fig.4) is very similar  
485 to that of BS, with a prevalence of Cryogenian and Ediacaran ages and occurrence of some  
486 Paleoproterozoic and Archean grains. Moreover, the whole-rock Sm-Nd isotopic signatures of  
487 samples from the Initial Red Beds give  $\epsilon_{Nd(T)}$  values and model ages (-4.4 – -3.0 and 1.4 – 1.5 Ga,  
488 respectively; Table 1) that fall within the range of the Brioverian sedimentary rocks (-1.4 – -6.2 and  
489 1.2 – 1.6 Ga, respectively). All these data are in agreement with local sources from the Armorican  
490 basement, i.e., Cadomian magmatic rocks and Brioverian sediments. The origin of Furongian (latest  
491 Cambrian) and Tremadocian (earliest Ordovician) zircon grains may be related to volcanism  
492 associated with episodes of continental rifting ( Guerrot et al., 1992; Auvray et al., 1980; Bonjour et  
493 al., 1988; Miller et al., 2001; Ballouard et al., 2018).

494

### 495 5.3. Grès Armoricaïn and overlying formations

496 There is a marked change of zircon populations from the Grès Armoricaïn Fm (GAFS, 1a,b in Fig.  
497 8) onwards. This is testified by the emergence of Stenian to Tonian >800 Ma grains (Fig. 4) whose  
498  $\epsilon_{Hf(t)}$  values range from -20 to 8 with a predominance of zircon grains with negative  $\epsilon_{Hf(t)}$  values (Fig.  
499 6). Moreover, the  $\epsilon_{Hf(t)}$  values of zircon with Tonian <800 Ma to Ediacaran ages are mostly negative  
500 (about -10 to -20) with Orosirian  $T_{DM}$  model ages, whereas the  $\epsilon_{Hf(t)}$  of the underlying sediments are



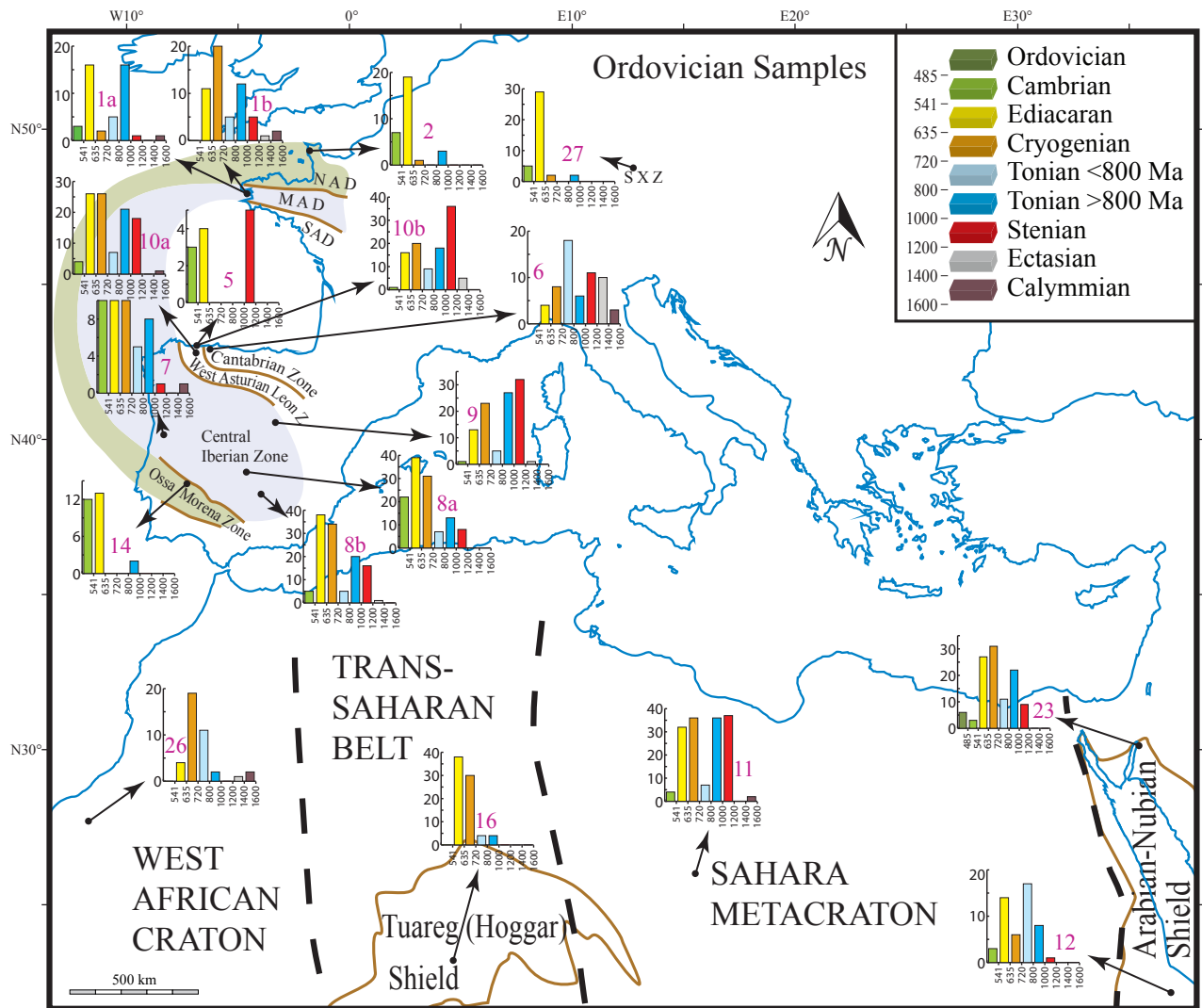
501 mostly positive with Ectasian and Stenian model ages. The whole-rock Sm-Nd isotopic signatures  
502 (Fig. 3) support the assumption of a significant change in source areas; old model ages (1.7 to 2.1 Ga  
503 versus 1.2 to 1.6 Ga) attest to supply of recycled crustal material.

504 The zircon grain age distribution is similar in the Middle-Upper Ordovician sample (PFS+KFS),  
505 with the only difference to GAFS observed in the amplitudes of the major peaks with a relative  
506 decrease of abundance of Tonian >800 Ma and Ediacaran ages and increase of grains with Cryogenian  
507 ages (main peak at 640 Ma). Detrital zircon grains of Tonian >800 Ma ages appear also in Normandy  
508 (2: Strachan et al., 2014, in Fig. 8) but they are less abundant and there are no Stenian zircon grains  
509 reported from there.

510 Since the detrital zircon grains of the Brioverian sample (BS) are of local origin (Fig. 6) represent  
511 a provenance older than the Cadomian orogenesis, our U-Pb-Hf isotopic results are relevant for the  
512 evolution of the Armorican crust in pre-Cadomian times. The Ordovician samples show the evolution  
513 of the sedimentary flux from respective source areas in more recent times, during the rifting that led  
514 to the opening of the Rheic Ocean. In Ordovician samples the sedimentary contribution changed due  
515 to Cadomian orogenesis. The new paleogeographic context provides, on the one hand, new  
516 populations (e.g., Stenian and Tonian >800Ma) and, on the other, a contribution of zircons that have  
517 the age population as the Brioverian sample (BS) - but with different  $\epsilon_{\text{Hf}(t)}$  values. In fact, we note  
518 that the  $\epsilon_{\text{Hf}(t)}$  values of the zircon grains of the BS and IRBS samples, which have relatively proximal  
519 source areas, are mostly positive, while the younger samples (GAFS and PFS+KFS) have mostly  
520 zircon with negative values (Fig. 6).

521

522



523

524 Fig. 8: Map with detrital zircon age spectra for Ordovician samples. Zircon population diagrams are  
 525 limited to the most significant age ranges, and the oldest Mesoproterozoic ages have been excluded  
 526 (>1600 Ma). Age spectra 1a and 1b are from this work (Fig. 4), the other diagrams were extracted  
 527 from the literature, as mentioned in the text.

528  
 529 Although the contribution from the Cadomian basement in the Armorican Massif cannot be totally  
 530 excluded for the Grès Armoricain Fm and overlying formations, external contributions must be  
 531 considered. Between the sedimentation of the Initial Red Beds and the sedimentation of the Upper  
 532 Ordovician formations, the environmental context of the MAD evolved from small isolated basins  
 533 developed above tilted blocks related to the Rheic opening, with local inputs, to a wide passive margin  
 534 setting along the northern Gondwana margin (Dauteuil et al., 1987; Brun et al., 1991). This resulted  
 535 in significant supply from terrigenous sediments overlying the Cadomian / Pan-African basement or  
 536 the Cambrian formations. According to the palaeocurrents, the origin of these sediments could be

537 found in the Gondwana hinterland (Beuf et al., 1971; Noblet and Lefort, 1990; Ghienne et al., 2007;  
538 Avigad et al., 2012). The source areas of the new zircon populations identified in the Grès Armoricaïn  
539 Fm and overlying formations of the MAD must then be investigated Gondwana wide. Within this  
540 continent, Neoproterozoic ages are known from many areas (e.g., Tuareg Shield, Mauritanide fold  
541 belt, East African Orogen) related to the Pan-African orogenic cycle from about 850 to 550 Ma  
542 (Liégeois et al., 1994, 2003; Abdelsalam et al., 2002; Küster et al., 2008). Several areas experienced  
543 magmatic events between late Mesoproterozoic and the early Neoproterozoic times (cf. maps and  
544 compilations in Linnemann et al., 2004, 2011; Pereira et al., 2012b; Fernández-Suárez et al., 2014;  
545 Shaw et al., 2014), e.g., the Sunsas Belt and Arequipa Massif at the southern Amazonian Craton, the  
546 Irumide and Kibaran belts (to the south and west of the Tanzania Craton), the Namaqua-Natal belt  
547 (southern Kaapvaal craton), and the Arabian-Nubian Shield. The palaeogeographic affinities of the  
548 MAD can be found in these geological domains that in the Ordovician time were supplied with a  
549 similar sedimentary flux, with zircon grains of Stenian Tonian >800 Ma and age.

550 The high textural and mineralogical maturity of the sedimentary rocks of the Grès Armoricaïn Fm  
551 (Dabard et al., 2007; Pistis et al., 2016) and the abraded and rounded forms of the majority of zircon  
552 grains in this formation are not in agreement with the rift context, in which this formation was laid  
553 down. These petrographic characteristics can be explained by the reworking of sandy sources, already  
554 mature and available on the Gondwana continent. A compilation of detrital zircon ages for North  
555 Africa and Western Europe was undertaken (Figs. 7 and 8). It shows that in North Africa, Stenian  
556 and Tonian >800 Ma ages are known from Neoproterozoic and Cambrian sedimentary rocks (Fig. 7)  
557 in the Arabian–Nubian Shield (Avigad et al., 2003; 12: Avigad et al., 2007; 13: Morag et al., 2012;  
558 24: Be’eri-Shlevin et al., 2009), the Saharan Metacraton (11: Meinhold et al., 2011; 29: Le Heron et  
559 al., 2009), and from some Cambrian samples of the West African Craton (Bradley et al., 2015; 25:  
560 Gärtner et al., 2017; 28: Avigad et al., 2012). Moreover, studies of some Neoproterozoic and  
561 Cambrian samples from the West African Craton have shown a total absence of Tonian and Stenian  
562 zircons (19: Abati et al., 2010; 20: Avigad et al., 2012).

563        Regarding Ordovician sediments (Fig. 8), these ages are present in the eastern zone, i.e., Arabian-  
564 Nubian Shield and Sahara Metacraton (23: Kolodner et al., 2006; 12: Avigad et al., 2007; 11:  
565 Meinhold et al., 2011). In contrast, only rare Tonian >800 Ma zircon grains occur in the western zone,  
566 i.e., the Tuareg Shield and West African Craton (16: Linnemann et al., 2011; 26: Gärtner et al., 2017).  
567 In Western Europe, Stenian and Tonian >800 Ma grains are not ubiquitous in Ordovician sediments.  
568 In the Iberian Massif, they are present with variable abundances in the West Asturian, Cantabrian and  
569 Central Iberian Zones (5: Fernández Suárez et al., 2000; 6: Fernández Suárez et al., 2002b; 7: Pereira  
570 et al., 2012a; 8, 9, 10: Shaw et al., 2014). In the Ossa Morena Zone (Iberian Massif; 14; Linnemann  
571 et al., 2008) and Saxo-Thuringia (27: Linnemann et al., 2008) only a few Tonian >800 Ma zircon  
572 grains have been noted.

573        Thus, the comparison of detrital zircon populations between the Armorican Massif and other areas  
574 along the North Gondwana margin shows similarities between the MAD and the Central Iberian,  
575 West Asturian and Cantabrian Zones, the Saharan Metacraton and the Arabian-Nubian Shield, on the  
576 one hand, and Normandy (2: NAD; Strachan et al., 2014), the Ossa Morena Zone, Saxo-Thuringia,  
577 the West African Craton, and the Tuareg Shield, on the other.

578        In palaeogeographic reconstructions, the Armorican Massif is often located to the north of the  
579 West African Craton (e.g. Linnemann et al., 2008; Avigad et al., 2012; Stephan et al., 2019).  
580 However, the occurrence of zircon populations of Stenian and late Tonian age in the Grès Armoricain  
581 Fm in the MAD excludes derivation from this basement. Moreover, available data on zircon  
582 populations of sediments laid down during Ordovician time in the Tuareg Shield (Linnemann et al.,  
583 2011) and on the West Africa Craton (Gärtner et al., 2016) emphasize the lack of zircon grains with  
584 Stenian and late Tonian ages. These features exclude that these zones and the MAD were in close  
585 proximity. By contrast, the similarities between detrital zircon populations from the MAD and those  
586 from the Arabian-Nubian Shield and Saharan Metacraton suggest possible relationships between  
587 these areas.

588 The generally juvenile character of the magmatism in the Arabian–Nubian Shield, demonstrated  
589 by  $\epsilon\text{Nd}(t)$  and  $\epsilon\text{Hf}(t)$  values (Hargrove et al., 2006; Morag et al., 2011), excludes this basement as the  
590 main source area for the zircon population with Stenian and Tonian >800 Ma ages. Considering that  
591 the sedimentary rocks of the Grès Armoricaire Fm are characterized by negative isotopic Sm-Nd  
592 signatures (Morag et al., 2011), they possibly are derived from reworking of the Cambro-Ordovician  
593 sedimentary cover of the Arabian–Nubian Shield or from the same source area that fed it. In this  
594 regard, some authors (Squire et al., 2006; Meinhold et al., 2013) proposed that the Cambrian-  
595 Ordovician sediments (e.g., Libya: Meinhold et al., 2011; Jordan: Kolodner et al., 2006) constituted  
596 a super-fan system, fed by erosion of the East African Orogen (also often referred as the  
597 Transgondwanan Supermountain). These sediments have age probability density distribution plots  
598 similar to those for the Armorican sedimentary rocks (two main zircon populations, one Pan-African  
599 and the other Stenian to late Tonian in age, separated by a gap around 800 Ma; cf. compilation in  
600 Meinhold et al., 2013 and Figs. 7 and 8).

601 This hypothesis implies that the MAD should be positioned further east along the Gondwana  
602 margin, likely to the north of the Saharan Metacraton and the Arabian-Nubian Shield. In the same  
603 way, the analysis of zircon grain populations of some areas of the Iberian Massif (NW Iberia, Central  
604 Iberian Zone) has already led some authors (Fernández-Suárez et al., 2014; Meinhold et al., 2013;  
605 Shaw et al., 2014; Stephan et al., 2019) to propose a location to the north of the Sahara Metacraton.  
606 By contrast, the Ordovician sample from Normandy (NAD), characterized by a lack of Stenian  
607 detrital zircon and a paucity of Tonian grains (Strachan et al., 2014), yielded a zircon population close  
608 to that of Saxo-Thuringia and in the Ossa Morena zone (Fig. 8). These findings attest to distinct  
609 source areas for the North and Medio Armorican Domains and demonstrate that these areas had to be  
610 distant from each other during the Lower Ordovician, and that they moved closer until they were fully  
611 connected in more recent times, probably during the Variscan orogenesis.

612

613 **6. Conclusion**

614 Detrital zircon age analysis of sedimentary rocks from the Medio Armorican Domain reveals a  
615 variation of source areas for the terrigenous flux between the Ediacaran and the Upper Ordovician  
616 times, highlighted by the addition of new populations of zircon ages to the populations of the  
617 comparatively older strata. Cryogenian and Ediacaran ages are dominant in the zircon populations of  
618 Brioverian sedimentary rocks that were mainly fed by the erosion of the Cadomian belt. The first  
619 Palaeozoic sedimentary strata (Initial Red Beds) have the same zircon populations provided from the  
620 erosion of the Brioverian rocks. In the Grès Armoricain Fm, zircon grains with Stenian and Tonian  
621 >800 Ma ages appear, and whole-rock Sm-Nd and zircon Hf isotopic signatures attest to a greater  
622 contribution of recycled crustal material and to a renewal of source areas. These sediments were laid  
623 down in a rift setting with high subsidence rates (the environment remained in tidal facies over several  
624 hundred meters thickness) that is in contrast to their high compositional and textural maturity. This  
625 paradox, isofacies deposition versus sediment maturity, can be explained by a sedimentary flux from  
626 a faraway origin. In the Cambro-Ordovician sediments of North Africa, zircon grains of Stenian and  
627 late Tonian ages are rare in the western part but they are ubiquitous in the eastern part (Saharan  
628 Metacraton, Arabian-Nubian Shield). Here, whole-rock Sm-Nd and zircon Hf isotopic signatures also  
629 attest to supply of recycled crustal material. These sediments, which according to Squire et al. (2006)  
630 and Meinhold et al. (2013) constituted a super-fan system, could be the source of the Ordovician  
631 sediments of the MAD. In this case, the MAD had to be positioned towards the Saharan Metacraton  
632 and the Arabian-Nubian Shield. The lack of Stenian and late Tonian ages in the zircon populations  
633 of Ordovician sediments of the NAD implies distinct source areas probably located further to the  
634 west.

635 On the basis of the presence or lack of Stenian and Tonian >800 Ma ages, the comparison of  
636 detrital zircon populations with the Iberian Massif shows for the Brioverian sediments similarities  
637 with the Ossa Morena Zone and, for the Ordovician sediments, similarities with the Central Iberian,  
638 West Asturian and Cantabrian zones. In contrast with the Armorican Massif, Stenian and Tonian  
639 >800 Ma zircon populations were present in these Iberian zones from the Ediacaran until the

640 Ordovician. During the Neoproterozoic, in the NW Iberian Massif some inputs came from the  
641 Arabian-Nubian Shield (Fernández-Suárez et al., 2014), whereas in the Armorican Massif the sources  
642 were constrained to the Cadomian basement. After the closure of the back-arc basin limiting the  
643 Armorican Massif and the Gondwana continent, the source area of the Ordovician sediments of the  
644 MAD would have been the super-fan system developed in eastern Gondwana, from where Stenian  
645 and Tonian >800 Ma zircon populations are known.

646

647

648

#### 649 *Acknowledgements*

650

651 Constructive comments by anonymous reviewers were greatly appreciated. The authors thank W.U.,  
652 Reimold and J.J., Peucat for scientific discussion. This work was supported by the “Fondazione  
653 Banco di Sardegna” and by the "Regione Autonoma della Sardegna" [grant numbers  
654 F74I19000960007, J81G17000110002]. The work of NH has been partially supported by Brazilian  
655 National Council for Scientific and Technological Development (CNPq) fellowships (grant  
656 309878/2019-5).

657

658

659

#### 660 **References**

- 661 Abati, J., Aghzer, M.A., Gerdes, A., Ennih, N., 2010. Detrital zircon ages of Neoproterozoic sequences of the  
662 Moroccan Anti-Atlas belt. *Precambrian Research* 181, 115-128.
- 663 Abdelsalam, M.G., Liégeois, J.P., Stern, R.J., 2002. The Saharan Metacraton. *Journal of African Earth*  
664 *Sciences* 34, 119–136.
- 665 Albarède, F., Telouk, P., Blichert-Toft, J., Boyet, M., Agranier, A., Nelson, B., 2004. Precise and accurate  
666 isotopic measurements using multiple-collector ICPMS. *Geochimica et Cosmochimica Acta* 68, 2725–  
667 2744.
- 668 Auvray, B., 1979. Genèse et évolution de la croûte continentale dans le Nord du Massif Armoricaïn. Thèse  
669 d’Etat, Université Rennes, 680 pp.

- 670 Auvray, B., Charlot, R., Vidal, P., 1980. Données nouvelles sur le Protérozoïque inférieur du domaine Nord-  
671 Armoricaïn (France): âge et signification. *Canadian Journal of Earth Sciences* 17, 532-538.
- 672 Avigad, D., Kolodner, K., McWilliams, M., Persing, H., Weissbrod, T., 2003. Origin of northern Gondwana  
673 Cambrian sandstones revealed by detrital zircon SHRIMP dating. *Geology* 31, 3, 227-230.
- 674 Avigad, D., Stern, R.J., Beyth, M., Miller, N., McWilliams, M.O., 2007. Detrital zircon U–Pb geochronology  
675 of Cryogenian diamictites and Lower Paleozoic sandstone in Ethiopia (Tigrai): Age constraints on  
676 Neoproterozoic glaciation and crustal evolution of the southern Arabian–Nubian Shield. *Precambrian  
677 Research* 154, 88-106.
- 678 Avigad, D., Gerdes, A., Morag, N., Bechstädt, T., 2012. Coupled U–Pb–Hf of detrital zircons of Cambrian  
679 sandstones from Morocco and Sardinia: Implications for provenance and Precambrian crustal evolution of  
680 North Africa. *Gondwana Research* 21, 690-703.
- 681 Ballouard, C., Poujol, M., Zeh, A., 2018. Multiple crust reworking in the French Armorican Variscan belt:  
682 implication for the genesis of uranium-fertile leucogranites. *International Journal of Earth Sciences* 107,  
683 2317–2336.
- 684 Be'eri-Shlevin, Y., Katzir, Y., Whitehouse, M.J., Kleinhanns, I.C., 2009. Contribution of pre Pan-African crust  
685 to formation of the Arabian Nubian Shield: New secondary ionization mass spectrometry U-Pb and O  
686 studies of zircon. *Geology* 37, 10, 899-902.
- 687 Beuf, S., Biju-Duval, B., de Charpal, O., Rognon, P., Gariel, O., and Benacef, A., 1971. Les grès du Paléozoïque  
688 inférieur au Sahara. *Sédimentation et discontinuités. Evolution structurale d'un craton: Institut Français du  
689 Pétrole, Science et technique du Pétrole* 18, 464 pp.
- 690 Black, L. P., Calver, C. R., Seymour, D. B., & Reed, A., 2004. SHRIMP U–Pb detrital zircon ages from  
691 Proterozoic and Early Palaeozoic sandstones and their bearing on the early geological evolution of  
692 Tasmania. *Australian Journal of Earth Sciences*, 51, 6, 885-900.
- 693 Bonjour, J.-L., Peucat, J.-J., Chauvel, J.-J., Paris, F., Cornichet, J., 1988. U–Pb zircon dating of the Early  
694 Paleozoic (Arenigian) transgression in Western Brittany (France): anew constraint for the Lower Paleozoic  
695 time-scale. *Chemical Geology* 72, 329–336.
- 696 Bonjour, J.L., 1988. *Sédimentation paléozoïque initiale dans le Domaine Centre Armoricaïn*. Unpublished  
697 PhD Thesis, Université de Rennes I, France 257pp.
- 698 Bouvier, A., Vervoort, J.D., Patchett, P.J., 2008. The Lu–Hf and Sm–Nd isotopic composition of CHUR:  
699 constraints from unequilibrated chondrites and implication for the bulk composition of terrestrial planets.  
700 *Earth and Planetary Science Letters* 273, 48–57.
- 701 Bradley, D.C., O'Sullivan, P., Cosca, M.A., Motts, H.A., Horton, J.D., Taylor, C.D., Beaudoin, G., Lee, G.K.,  
702 Ramezani, J., Bradley, D.B., Jones, J.V., Bowring, S., 2015. Synthesis of geological, structural, and  
703 geochronologic data (Phase V, Deliverable 53). Chapter A of Taylor C.D. (ed.), *Second Projet de  
704 Renforcement Institutionnel du Secteur Minier de la République Islamique de Mauritanie (PRISM-II)*. U.S.  
705 Geological Survey Open-File Report 2013- 12080-A, 328p. doi:10.3133/ofr20131280.



706 Brun, J.P., Ballard, J.F., Le Corre, C., 1991. Identification of Ordovician block-tilting in the Hercynian fold-  
707 belt of Central Brittany (France): field evidence and computer models. *Journal of Structural Geology* 13,  
708 419–429.

709 Bühn, B., Pimentel, M.M., Matteini, M., Dantas, E.L., 2009. High spatial resolution analysis of Pb and U  
710 isotopes for geochronology by laser ablation multi-collector inductively coupled plasma mass spectrometry (L-  
711 C-ICPMS). *Anais da Academia Brasileira de Ciências* 81, 99-114.

712 Chantraine, J., Chauvel, J.J., Dupret, L., Gatinot, F., Icart, J.C., Le Corre, C., Rabu, D., Sauvan, P. and Villey,  
713 M., 1983. Inventaire lithologique et structural du Briovérien (Protérozoïque) de la Bretagne Centrale et du  
714 Bocage normand pour la recherche de guides métallogéniques. *Documents du Bureau de Recherches*  
715 *Géologiques et Minières* 67, 185 pp.

716 Chantraine, J., Autran, A., Cavelier, C., 1996. Carte géologique de la France, 1/1 000 000. BRGM, Orléans,  
717 France.

718 Chantraine, J., Houlgatte, E., Chauris, L., Coussement, C., Le Goff, E., Barrière, M., Larssonneur, C., Garreau,  
719 J., 1999. Carte Géologique de France (1/50 000), feuille Lannion (203), BRGM, Orléans. Explanatory notes  
720 by Chantraine et al., 144 pp.

721 Chantraine, J., Egal, E., Thiéblemont, D., Le Goff, E., Guerrot, C., Ballèvre, M., Guennoc, P., 2001. The  
722 Cadomian active margin (North Armorican Massif, France): a segment of the North Atlantic Panafrikan  
723 belt. *Tectonophysics* 331, 1-18.

724 Chauvel, C., Blichert-Toft, J., 2001. A hafnium isotope and trace element perspective on melting of the  
725 depleted mantle. *Earth and Planetary Science Letters* 190, 137–151, doi:10.1016/S0012-821X(01)00379-  
726 X.

727 Cocherie, A., Chantraine, J., Mark Fanning, C., Dabard, M.P., Paris, F., Le Hérissé, A., Egal, E., 2001. Datation  
728 U/Pb: âge Briovérien de la série d'Erquy (Massif armoricain, France). *Comptes Rendus de l'Académie des*  
729 *Sciences, Paris* 333, 427-434.

730 Dabard, M.P., 1990. Lower Brioverian formations (Upper Proterozoic) of the Armorican Massif (France):  
731 geodynamic evolution of source areas revealed by sandstone petrography and geochemistry. *Sedimentary*  
732 *Geology* 69, 45-58.

733 Dabard, M.P., Loi, A., Peucat, J.J., 1996. Zircon typology combined with Sm-Nd whole-rock isotope analysis  
734 to study Brioverian sediments from the Armorican Massif. *Sedimentary Geology* 101, 243-260.

735 Dabard, M.P., 2000. Petrogenesis of graphitic cherts in the Armorican segment of the Cadomian orogenic belt  
736 (NW France). *Sedimentology* 47, 787-800.

737 Dabard, M.P., Loi, A., Paris, F., 2007. Relationship between phosphogenesis and sequence architecture:  
738 sequence stratigraphy and biostratigraphy in the Middle Ordovician of the Armorican Massif (France).  
739 *Palaeogeography, Palaeoclimatology, Palaeoecology* 248, 339-356.

740 Dabard, M.P., Loi, A., Paris, F., Ghienne, J.F., Pistis, M., Vidal, M., 2015. Sea-level curve for the Middle to  
741 early Late Ordovician in the Armorican Massif (western France): Icehouse third-order glacio-eustatic  
742 cycles. *Palaeogeography, Palaeoclimatology, Palaeoecology* 436, 96-111.

743 Dauteuil O., Durand J., Brun J.-P., 1987. Arguments en faveur de décrochements synchrones du dépôt des  
744 séries rouges d'Erquy-Fréhel. Comptes Rendus de l'Académie des Sciences, Paris, II-304, 83-88.

745 Denis, E., Dabard, M.P., 1988. Sandstone petrography and geochemistry of Late Proterozoic sediments of the  
746 Armorican Massif (France) – A key to basin development during the Cadomian orogeny. Precambrian  
747 Research 42, 189-206.

748 DePaolo, D.J., 1981. Neodymium isotopes in the Colorado Front Range and crust-mantle evolution in the  
749 Proterozoic. Nature 291, 193–196.

750 Egal, E., Guerrot, C., Le Goff E., Thiéblenont, D., Chantraine, J., 1996. The Cadomian orogeny revisited in  
751 northern Brittany (France). Geological Society of America Special Paper 304, 281-318.

752 Fernández-Suárez, J., Gutiérrez Alonso, G., Jenner, G.A., Tubrett, M.N., 2000. New ideas on the Proterozoic-  
753 Early Palaeozoic evolution of NW Iberia: insights from U-Pb detrital zircon ages. Precambrian Research  
754 102, 185-206.

755 Fernández-Suárez, J., Gutiérrez Alonso, G., Jeffries, T.E., 2002a. The importance of along-margin terrane  
756 transport in northern Gondwana: insights from detrital zircon parentage in Neoproterozoic rocks from Iberia  
757 and Brittany. Earth and Planetary Science Letters 204, 75-88.

758 Fernández-Suárez, J., Gutiérrez Alonso, G., Cox, R., Jenner, G.A., 2002b. Assembly of the Armorica  
759 Microplate: A Strike-Slip Terrane Delivery? Evidence from U-Pb Ages of Detrital Zircons. The Journal of  
760 Geology 110, 619–626.

761 Fernández-Suárez, J., Gutiérrez Alonso, G., Pastor-Galán, D., Hofmann, M., Murphy, J.B., Linnemann, U.,  
762 2014. The Ediacaran-Early Cambrian detrital zircon record of NW Iberia: possible sources and  
763 paleogeographic constraints. International Journal of Earth Sciences 103, 1335-1357.

764 Gapais, D., Le Corre, C., 1980. Is the Hercynian belt of Brittany a major shear zone. Nature 288, 574-576.

765 Gärtner, A., Villeneuve, M., Linnemann, U., Gerdes, A., Youbi, N., & Hofmann, M., 2016. Similar crustal  
766 evolution in the western units of the Adrar Souttoug Massif (Moroccan Sahara) and the Avalonian terranes:  
767 Insights from Hf isotope data. Tectonophysics 681, 305-317.

768 Gärtner, A., Youbi, N., Villeneuve, M., Sagawe, A., Hofmann, M., Mahmoudi, A., Boumehdi, M. A.,  
769 Linnemann, U., 2017. The zircon evidence of temporally changing sediment transport-the NW Gondwana  
770 margin during Cambrian to Devonian time (Aoucert and Smara areas, Moroccan Sahara). International  
771 Journal of Earth Sciences (Geol Rundsch) doi: 10.1007/s00531-017-1457-x

772 Gerdes A., Zeh A., 2006. Combined U-Pb and Hf isotope LA-(MC)-ICP-MS analyses of detrital zircons:  
773 comparison with SHRIMP and new constraints for the provenance and age of an Armorican metasediment  
774 in Central Germany. Earth and Planetary Science Letters 249, 47-61.

775 Gerdes A., Zeh A., 2009. Zircon formation *versus* zircon alteration - New insights from combined U-Pb and  
776 Lu-Hf *in-situ* LA-ICP-MS analyses, and consequences for the interpretation of Archean zircon from the  
777 Central Zone of the Limpopo Belt. Chemical Geology 261, 230-243.

778 Ghienne, J.-F., Boumendjel, K., Paris, F., Videt, B., Racheboeuf, P., Ait Salem, H., 2007. The Cambrian–  
779 Ordovician succession in the Ougarta Range (western Algeria, North Africa) and interference of the Late

780 Ordovician glaciation on the development of the Lower Palaeozoic transgression on northern Gondwana.  
781 Bulletin of Geosciences 82, 3, 183–214.

782 Gorini, A., Vidal, M., Loi, A., Paris F., 2008. Evoluzione stratigrafica pre-hirnantiana della Formazione di  
783 Kermeur (Massiccio Armoricano). Rendiconti Online Societa Geologica Italiana 3, 2, 451-452.

784 Gougeon, R., Néraudeau, D., Dabard, M.P., Pierson-Wieckmann, A.C., Polette, F., Poujol, M., Saint-Martin,  
785 J.P., 2018. Trace Fossils from the Brioverian (Ediacaran–Fortunian) in Brittany (NW France). Ichnos 25,  
786 1, 11-24. doi: 10.1080/10420940.2017.1308865.

787 Graviou, P., Peucat, J.J., Auvray, B., Vidal, P., 1988. The Cadomian orogeny in the northern Armorican  
788 Massif. Petrological and geochronological constraints on a geodynamic model. Hercynica IV, 1, 1-13.

789 Guerrot, C., Peucat, J.J., 1990. U-Pb geochronology of the late Proterozoic Cadomian Orogeny in the Northern  
790 Armorican Massif, France. In: RS. D'Lemos, R.A. Strachan and C.G. Topley (Editors), The Cadomian  
791 Orogeny. Geological Society of London, Special Publication 51, 13-26.

792 Guerrot, C., Calvez, J.Y., Bonjour, J.L., Chantraine, J., Chauvel, J.J., Dupret, L., Rabu, D., 1992. Le Briovérien  
793 de Bretagne centrale et occidentale : nouvelles données radiométriques. Comptes Rendus de l'Académie  
794 des Sciences 315, 1741-1746.

795 Hargrove, U.S., Stern, R.J., Kimura, J.-I., Manton, W.I., Johnson, P.R., 2006. How juvenile is the Arabian–  
796 Nubian Shield? Evidence from Nd isotopes and pre-Neoproterozoic inherited zircon in the Bi'r Umq suture  
797 zone, Saudi Arabia. Earth and Planetary Science Letters 252, 308–326.

798 Hebert, R., Hallot, E., Guerrot, C., Chantraine, J., 1993. New structural, petrological and radiometric  
799 constraints within the Cadomian belt: chronology of events in the baie de Saint Brieuc, Northern Armorican  
800 Massif (France). Comptes Rendus de l'Académie des Sciences, Paris 316, II, 395-401.

801 Horstwood, M.S., Košler, J., Gehrels, G., Jackson, S.E., McLean, N.M., Paton, C., ..., Bowring, J.F., 2016.  
802 Community-derived standards for LA-ICP-MS U-(Th-) Pb geochronology–Uncertainty propagation, age  
803 interpretation and data reporting. Geostandards and Geoanalytical Research, 40, 3, 311-332.

804 Inglis, J.D., Samson, S.D., D'Lemos, R.S., Hamilton, M., 2004. U–Pb geochronological constraints on the  
805 tectonothermal evolution of the Paleoproterozoic basement of Cadomia, La Hague, NW France.  
806 Precambrian Research 134, 293-315.

807 Inglis, J.D., Samson, S.D., D'Lemos, R.S., Miller, B.V., 2005. Timing of Cadomian deformation and  
808 magmatism within La Hague, NW France. Journal of the Geological Society, London 162, 389–400.

809 Jackson, S.E., Pearson, N.J., Griffin, W.L., Belousova, E.A., 2004. The application of laser ablation-  
810 inductively coupled plasma-mass spectrometry to in situ U-Pb zircon geo- chronology. Chemical Geology  
811 211, 47–69.

812 Jahn, B.M., Bernard-Griffiths, J., Chariot, R., Cornichet, J., Vidal, P., 1980. Nd and Sr isotopic compositions  
813 and REE abundances of Cretaceous MORB (Holes 417D and 418A, Legs 51, 52 and 53). Earth and  
814 Planetary Science Letters 48, 103-124.

815 Jégouzo, P., 1980. The South Armorican Shear Zone. Journal of Structural Geology 2, 1-2, 39-47.

816 Kolodner, K., Avigad, D., McWilliams, M., Wooden, J.L., Weissbrod, T., Feinstein, S., 2006. Provenance of  
817 north Gondwana Cambrian-Ordovician sandstone: U-Pb SHRIMP dating of detrital zircons from Israel and  
818 Jordan. *Geological Magazine* 143, 367-391.

819 Kosler, J., Fonneland, H., Sylvester, P., Tubrett, M., Pedersen, RB., 2002. U-Pb dating of detrital zircons for  
820 sediment provenance studies - a comparison of laser ablation ICMPS and SIMS techniques. *Chemical*  
821 *Geology* 182, 605-618.

822 Küster, D., Liégeois, J.P., Matukov, D. Sergeev, S., Lucassen, F., 2008. Zircon geochronology and Sr, Nd, Pb  
823 isotope geochemistry of granitoids from Bayuda Desert and Sabaloka (Sudan): Evidence for a Bayudian  
824 event (920–900 Ma) preceding the Pan-African orogenic cycle (860–590 Ma) at the eastern boundary of  
825 the Saharan Metacraton. *Precambrian Research* 164, 16–39.

826 Le Corre, C., 1977. Le Briovérien de Bretagne centrale: essai de synthèse lithologique et structurale. *Bulletin*  
827 *du Bureau de Recherche Géologique et Minière* I, 3, 219-254.

828 Le Heron, D.P., Howard, J.P., Alhassi, A.M., Anderson, L.M., Morton, A.C., Fanning, C.M., 2009. Field-  
829 based investigations of an ‘Infracambrian’ clastic succession in SE Libya and its bearing on the evolution  
830 of the Al Kufrah Basin. In: Craig, J., Thurow, J., Thusu, B., Whitham, A.G., Abutarruma, Y. (Eds.), *Global*  
831 *Neoproterozoic Petroleum Systems: The Emerging Potential in North Africa: Geological Society of London,*  
832 *Special Publication* 326, 193–210.

833 Liégeois, J.P., Black, R., Navez, J., Latouche, L., 1994. Early and late Pan-African orogenies in the Aïr  
834 assembly of terranes (Tuareg shield, Niger). *Precambrian Research* 67, 1-2, 59-88.

835 Liégeois, J.P., Latouche, L., Boughara, M., Navez, J., Guirad, M., 2003. The LATEA metacraton (Central  
836 Hoggar, Tuareg shield, Algeria): behaviour of an old passive margin during the Pan-African orogeny.  
837 *Journal of African Earth Sciences* 37, 161–190.

838 Linnemann, U., McNaughton, N.J., Romer, R.L., Gehmlich, M., Drost, K., Tonk, C., 2004. West African  
839 provenance for Saxo-Thuringia (Bohemian Massif): Did Armorica ever leave pre-Pangean Gondwana? -  
840 U/Pb-SHRIMP zircon evidence and the Nd-isotopic record. *International Journal of Earth Sciences* 93, 5,  
841 683-705.

842 Linnemann, U., Pereira, M.F., Jeffries, T., Drost, K., Gerdes, A., 2008. Cadomian Orogeny and the opening  
843 of the Rheic Ocean: new insights in the diachrony of geotectonic processes constrained by LA-ICP-MS U-  
844 Pb zircon dating (Ossa-Morena and Saxo-Thuringian Zones, Iberian and Bohemian Massifs).  
845 *Tectonophysics* 461, 21–43.

846 Linnemann, U., Ouzegane, K., Drareni, A., Hofmann, M., Becker, S., Gärtner, A., Sagawe, A., 2011. Sands  
847 of West Gondwana: An archive of secular magmatism and plate interactions-A case study from the  
848 Cambro-Ordovician section of the Tassili Ouan Ahaggar (Algerian Sahara) using U-Pb-La-ICP-MS detrital  
849 zircon ages. *Lithos* 123, 188-203.

850 Linnemann, U., Gerdes, A., Hofmann, M., Marko, L., 2014. The Cadomian Orogen: Neoproterozoic to Early  
851 Cambrian crustal growth and orogenic zoning along the periphery of the West African Craton-Constraints  
852 from U-Pb zircon ages and Hf isotopes. *Precambrian Research* 244, 236-278.

853 Marcoux, E., Cocherie, A., Ruffet, G., Darboux, J.R., Guerrot, C., 2009. Géochronologie revisitée du dôme du  
854 Léon (Massif armoricain, France). *Géologie de la France* 1, 19-40.

855 Martin, E., François, C., Paquette, J.L., Capdevila, R., Lejeune, A.M., 2018. Petro-geochemistry and zircon  
856 U-Pb dating of the late Variscan Flamanville granodiorite and its Paleoproterozoic basement (Normandy,  
857 France). *Géologie de la France* 1, 34-48.

858 Matteini, M., Dantas, E., Pimentel, M., Bühn, B., 2010. Combined U-Pb and Lu-Hf isotope analyses by laser  
859 ablation MC-ICP-MS: methodology and applications. *Annals of the Brazilian Academy of Science* 82(2),  
860 479-491.

861 Meinhold, G., Morton, A.C., Fanning, C.M., Frei, D., Howard, J.P., Phillips, R.J., Strogon, D., Whitham, A.G.,  
862 2011. Evidence from detrital zircons for recycling of Mesoproterozoic and Neoproterozoic crust recorded  
863 in Paleozoic and Mesozoic sandstones of southern Libya. *Earth and Planetary Science Letters* 312, 164-  
864 175.

865 Meinhold, G., Morton, A.C., Avigad, D., 2013. New insights into peri-Gondwana paleogeography and the  
866 Gondwana super-fan system from detrital zircon U-Pb ages. *Gondwana Research* 23, 661-665.

867 Michard, A., Gurriet, P., Soudant, M., Albarede, F., 1985. Nd isotopes in French Phanerozoic shales: external  
868 vs. internal aspects of crustal evolution. *Geochimica Cosmochimica Acta* 49, 601-610.

869 Miller, B.V., Samson, S.D., D'Lemos, R.S., 2001. U-Pb geochronological constraints on the timing of  
870 plutonism, volcanism and sedimentation, Jersey, Channel Island, UK. *Journal of the Geological Society,*  
871 *London* 158, 243-252.

872 Morag, N., Avigad, D., Gerdes, A., Belousova, E., Harlavan, Y., 2011. Detrital zircon Hf isotopic composition  
873 indicates long-distance transport of North Gondwana Cambrian-Ordovician sandstones. *Geology* 39, 10,  
874 955-958.

875 Morag, N., Avigad, D., Gerdes, A., Harlavand, Y., 2012. 1000–580 Ma crustal evolution in the northern  
876 Arabian-Nubian Shield revealed by U–Pb–Hf of detrital zircons from late Neoproterozoic sediments (Elat  
877 area, Israel). *Precambrian Research* 208–211, 197–212. doi.org/10.1016/j.precamres.2012.04.009.

878 Morel, M.L.A., Nebel, O., Nebel-Jacobsen, Y.J., Miller, J.S., Vroon, P.Z., 2008. Hafnium isotope  
879 characterization of the GJ-1 zircon reference material by solution and laser-ablation MC-ICPMS. *Chemical*  
880 *geology* 255, 1-2, 231-235.

881 Nagy, E., Samson, S.D., D'Lemos, R.S., 2002. U–Pb geochronological constraints on the timing of Brioverian  
882 sedimentation and regional deformation in the St. Brieuc region of the Neoproterozoic Cadomian orogen,  
883 northern France. *Precambrian Research* 116, 1–17

884 Nebel, O., Nebel-Jacobsen, Y., Mezger, K., Berndt, J., 2007. Initial Hf isotope compositions in magmatic  
885 zircon from early Proterozoic rocks from the Gawler Craton, Australia: A test for zircon model ages.  
886 *Chemical Geology* 241, 23-37.

887 Noblet, C., Lefort, J.P., 1990. Sedimentological evidence for a limited separation between Armorica and  
888 Gondwana during the Early Ordovician. *Geology* 18, 303-306.

889 Paris, F., Robardet, M., 1977. Paléogéographie et relations Ibéro-Armoricaines au Paléozoïque ante  
890 Carbonifère. *Bulletin de la Société Géologique de France* 7, 19, 1121-1126.

891 Paris, F., Robardet, M., Dabard, M.P., Feist, R., Ghienne, J.F., Guillocheau, F., Le Hérissé, A., Loi, A., Mélou,  
892 M., Servais, T., Shergold, J., Vidal, M., Vizcaïno, D., 1999. Ordovician sedimentary rocks of France. *Acta*  
893 *Universitatis Carolinae-Geologica* 43, 1/2, 85-88.

894 Pasteel, P., Doré, F., 1982. Age of the Vire-Carolles granite. In: G.S. Odin (Edit), *Numerical dating in*  
895 *stratigraphy*. Vol. II, NDS 212, 784-790.

896 Pereira, M.F., Linnemann, U., Hofmann, M., Chichorro, M., Solád, A.R., Medina, J., Silva, J.B., 2012a. The  
897 provenance of Late Ediacaran and Early Ordovician siliciclastic rocks in the Southwest Central Iberian  
898 Zone: Constraints from detrital zircon data on northern Gondwana margin evolution during the late  
899 Neoproterozoic. *Precambrian Research* 192–195, 166–189.

900 Pereira, M.F., Solád, A.R., Chichorro, Lopes, L.n Gerdes, A., Silva, J.B., 2012b. North-Gondwana assembly,  
901 break-up and paleogeography: U–Pb isotope evidence from detrital and igneous zircons of Ediacaran and  
902 Cambrian rocks of SW Iberia. *Gondwana Research* 22, 3-4, 866–881.

903 Peucat, J.J., Hirbec, Y., Auvray, B., Cogné, J., Cornichet, J., 1981. Late Proterozoic age from a basic-ultrabasic  
904 volcanic complex: a possible Cadomian orogenic complex in the Hercynian belt of western Europe.  
905 *Geology* 9, 169-173.

906 Peucat, J.J., 1986. Behaviour of Rb-Sr whole-rock and U-Pb zircon systems during partial melting as shown  
907 in migmatitic gneisses from the St-Malo massif, NE Brittany, France. *Journal of the Geological Society*  
908 143, 875-886.

909 Pistis, M., Loi, A., Dabard, M.P., 2016. Influence of relative sea-level variations on the genesis of  
910 palaeoplacers, the examples of Sarrabus (Sardinia, Italy) and the Armorican Massif (Western France).  
911 *Comptes Rendus Geoscience* 348, 150–157. doi 10.1016/j.crte.2015.09.006

912 Robardet, M., 2002. Alternative approach to the Variscan Belt in southwestern Europe: Preorogenic  
913 paleobiogeographical constraints. In: Martinez Catalan, J.R., Hatcher, R.D., Arenas, R., Diaz Garcia, F.  
914 (Eds.), *Variscan-Appalachian Dynamics: The Building of the Late Paleozoic Basement*. Geological Society  
915 of America Special Paper 364, 1-15.

916 Samson, S.D., D’Lemos, R.S., 1998. U-Pb geochronology and Sm-Nd isotopic composition of Proterozoic  
917 gneisses, Channel Islands, UK. *Journal of the Geological Society, London* 155, 609-618.

918 Samson, S.D., D’Lemos, R., Blichert-Toft, J., Vervoort, J., 2003. U-Pb geochronology and Hf-Nd isotope  
919 compositions of the oldest Neoproterozoic crust within the Cadomian orogen: new evidence for a unique  
920 juvenile terrane. *Earth and Planetary Science Letters* 208, 165-180.

921 Samson, S.D., D’Lemos, R., Miller, B.V., Hamilton, M.A., 2005. Neoproterozoic palaeogeography of the  
922 Cadomia and Avalon terranes: constraints from detrital zircon U–Pb ages. *Journal of the Geological*  
923 *Society, London* 162, 65–71.

924 Scherer, E., Münker, C., Mezger, K., (2001). Calibration of the lutetium-hafnium clock. *Science* 293, 5530,  
925 683-687.

- 926 Shaw, J., Gutiérrez-Alonso, G., Johnston, S.T., Pastor Galán, D., 2014. Provenance variability along the Early  
927 Ordovician north Gondwana margin: Paleogeographic and tectonic implications of U-Pb detrital zircon  
928 ages from the Armorican Quartzite of the Iberian Variscan belt. *Geological Society of America Bulletin*  
929 126, 5/6, 702–719, doi:10.1130/B30935.1.
- 930 Sláma, J., Košler, J., 2012. Effects of sampling and mineral separation on accuracy of detrital zircon studies.  
931 *Geochemistry, Geophysics, Geosystems* 13, 5, 17pp.
- 932 Squire, R.J., Campbell, I.H., Allen, C.M., Wilson, C.J.L., 2006. Did the Transgondwanan Supermountain  
933 trigger the explosive radiation of animals on Earth? *Earth and Planetary Science Letters* 250, 116–133.
- 934 Stephan, T., Kroner, U., Romer, R.L., 2019. The pre-orogenic detrital zircon record of the Peri-Gondwanan  
935 crust. *Geological Magazine* 156, 281–307.
- 936 Strachan, R.A., D’Lemos, R.S., Dallmeyer, R.D., 1996. Neoproterozoic evolution of an active plate margin:  
937 North Armorican Massif, France. In: Nance RD, Thompson MD (eds) *Avalonian and Related Peri-*  
938 *Gondwanan Terranes of the Circum-Atlantic*. Geological Society of America, Special Paper 304, 319-332.
- 939 Strachan, R.A., Linnemann, U., Jeffries, T., Drost, K., Ulrich, J., 2014. Armorican provenance for the mélange  
940 deposits below the Lizard ophiolite (Cornwall, UK): evidence for Devonian obduction of Cadomian and  
941 Lower Palaeozoic crust onto the southern margin of Avalonia. *International Journal of Earth Sciences (Geol*  
942 *Rundsch)* 103, 1359-1383, Doi 10.1007/s00531-013-0961-x.
- 943 Suire, P., Dabard, M.P., Chauvel, J.J., 1991. Nouvelles données sur les séries rouges nord-armoricaines : étude  
944 du bassin ordovicien de Bréhec. *Comptes Rendus de l’Académie des Sciences, Paris* 312, II, 721-727.
- 945 Talavera, C., Martínez Poyatos, D., González Lodeiro, F., 2015. SHRIMP U–Pb geochronological constraints  
946 on the timing of the intra-Alcudian (Cadomian) angular unconformity in the Central Iberian Zone (Iberian  
947 Massif, Spain). *International Journal of Earth Sciences (Geol Rundsch)* 104, 1739-1757, doi  
948 10.1007/s00531-015-1171-5.
- 949 Taylor, S.R., McLennan, S.M., 1985. *The Continental Crust: its Composition and Evolution*. Oxford: Black-  
950 well, 312 pp.
- 951 Thiéblemont, D., Egal, E., Guerrot, C., Chantraine, J., 1999. Témoins d’une subduction « éocadomienne »  
952 (665-655 Ma) en Bretagne nord: arguments géochimiques. *Géologie de la France* 1, 3-11.
- 953 Vidal P., Deutsch S., Martineau F., Cogné J., 1974. Nouvelles données radiométriques en Baie de Saint-Brieuc.  
954 Le problème d'un socle antécadomien nord-armoricain. *Comptes Rendus de l’Académie des Sciences,*  
955 *Paris*, 279, 631-634.
- 956 Vidal, P., 1980. L’évolution polyorogénique du Massif armoricain : apport de la géochronologie et de la  
957 géochimie isotopique du strontium. *Mémoire de la Société Géologique et Minéralogique de Bretagne* 21,  
958 162 pp.
- 959 Vidal, M., Dabard, M.P., Gourvenec, R., Le Hérisse, A., Loi, A., Paris, F., Plusquellec, Y., Racheboeuf, P.,  
960 2011a. Le Paléozoïque de la presqu’île de Crozon (France). *Géologie de la France* 1, 3–45.
- 961 Vidal, M., Loi, A., Dabard, M.P., Botquelen, A., 2011b. A Palaeozoic open shelf benthic assemblage in a  
962 protected marine environment. *Palaeogeography, Palaeoclimatology, Palaeoecology* 306, 27-40.

- 963 Wedepohl, K.H., 1995. The compositions of the continental crust. *Geochimica et Cosmochimica Acta* 59,  
964 1217-1232.
- 965 Young, T.P., 1988. The lithostratigraphy of the upper Ordovician of central Portugal. *Journal of the Geological*  
966 *Society of London* 145, 3, 377-392. doi.org/10.1144/gsjgs.145.3.0377.